Clin Neuroradiol (2020) (Suppl 1) 30:S1–S36
https://doi.org/10.1007/s00062-020-00951-w

55. Jahrestagung der Deutschen Gesellschaft für Neuroradiologie e. V.

Virtuelle Konferenz

Wissenschaftliche Leitung
Prof. Dr. Horst Urbach (Freiburg)

Dieses Supplement wurde von der Deutschen Gesellschaft für Neuroradiologie finanziert.

Online publiziert: 23 September 2020

Inhaltsverzeichnis

Video-Podcasts/Powerpitches

[3] Favorable Venous Microvascular Profile is Associated with Smaller Ischemic Lesion Growth and Smaller Final Core Infarction Volume in Patients with Acute Ischemic Stroke Due to Large Vessel Occlusion

TD Faizy[1,3], R Kabiri[1,3], M Leipzig[1], S Christensen[2], G Broocks[3], F Flottmann[3], U Hanning[3], M Lansberg[2], G Albers[2], J Fiehler[3], M Wintermark[1], JJ Heit[1]

[1]Department of Radiology, Stanford University School of Medicine, CA
[2]Department of Neurology and Neurological Sciences, Stanford University School of Medicine, CA
[3]Department of Neuroradiology, University Medical Center Hamburg-Eppendorf, Germany

Purpose: In the event of an acute ischemic stroke due to large vessel occlusion (AIS-LVO), patients with large core infarction and malignant edema have worse outcomes. Core infarction size growth is caused by poor cerebral blood flow and impaired microvascular perfusion. Cerebral microvascular perfusion is governed by the in-flow of arterial blood to the brain tissue, but also likely by the outflow of blood through the cerebral veins. Venous blood flow in the context of AIS-LVO may better indicate the overall quality of tissue perfusion, as it reflects blood flow after passing the brain tissue. We determined if the venous microperfusion profile (VMP) predict ischemic lesion growth and final infarct core in AIS-LVO patients.
Materials and Methods: We performed a multicenter, retrospective cohort study of AIS-LVO patients undergoing thrombectomy triage with CT angiography (CTA) and CT perfusion (CTP). Patients with motion artifact and incomplete electronical medical data were excluded. Patient details were obtained from prospectively maintained stroke databases and the electronic medical record. VMP was determined by opacification of the vein of Labbé, sphenoparietal sinus, and superficial middle cerebral vein on pre-thrombectomy CTA as: 0, not visible; 1, moderate opacification; and 2, full. Brain edema progression and infarct growth as assessed by Net Water Uptake (NWU), which was calculated on pre-treatment and post-thrombectomy non contrast computed tomography images using manual regions of interest. Primary outcome measure was ischemic lesion growth after thrombectomy. Secondary outcome was final core infarction volume, which was manually segmented on follow-up CT and MRI studies 24–48 h after thrombectomy.
Results: 250 patients met inclusion criteria. Median patient age was 76 (IQR 65–82). 50 % were female. Linear regression models found that increased patient age ($p=0.011$), higher blood glucose levels ($p=0.007$), lower TICI scores ($p<0.001$) and reduced VMP ($p<0.001$) predicted increased core infarction growth (higher NWU). In a multivariate regression analysis, poor VMP predicted core infarct growth while controlling for age, blood glucose, and TICI score ($\beta=-02.111840$, [95 % CI –02.808059256 –01.41562150]; $p<001$). In a secondary analysis focused on final infarct core, we excluded 5 patients due to missing final infarct size data. After controlling for age, blood glucose, and TICI score, poor VMP predicted higher final core infarct size ($\beta=-22.57626$, [95 % CI –30.7799325 –14.3725813]; $p<001$).
Conclusion: Poor cerebral perfusion on the venous microvascular profile predicts ischemic lesion growth and final infarct core volume in AIS-LVO patients treated with thrombectomy.

[5] Deep Brain Stimulation-Electrodes May Rotate After Implantation–An Animal Study

Rau A[1], Urbach H[1], Coenen VA[2], Egger K[1], Reinacher PC[2,3]

[1]Department of Neuroradiology, University Medical Center Freiburg
[2]Department of Stereotactic and Functional Neurosurgery, University Medical Center Freiburg
[3]Fraunhofer Institute for Laser Technology, Aachen, Germany

Background & Purpose: Directional Deep Brain Stimulation (dDBS) electrodes allow to steer the electrical field in a specific direction. When implanted with torque they may rotate for a certain time after implantation. Aim of this study was to evaluate whether and to which degree leads rotate in the first 24 h after implantation using a sheep brain model.

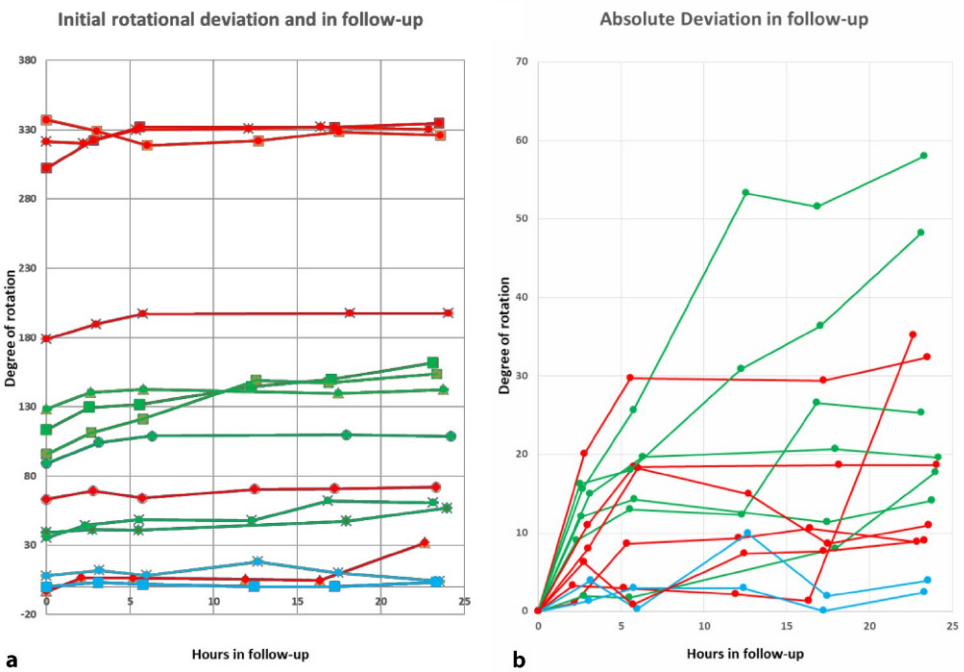

Fig. 1 Rotational deviation of implanted electrodes after applied torsion 180° applied torsion depicted in GREEN, 360° in RED and controls (0°) in BLUE. **a** Initial rotational deviation (timepoint 0 h) and in follow-up. **b** Absolute deviation in relation to the rotation after applied torsion

Methods: dDBS electrodes were implanted in 14 sheep heads and 3D rotational fluoroscopy (3D-RF) scans were acquired to visualize the orientation of the electrode leads according to Reinacher et al. 2017. Electrode leads were clockwise rotated just above the burrholes (180° $n=6$, 360° $n=6$, 2 controls) and 3D-RF scans were again acquired after three, six, 13, 17 and 24 h, respectively.
Results: 180° rotated electrodes showed an initial rotation of 83.5° (range: 35.4–128.3°) and a rotation of 114.0° (range: 57–162°) after 24 h. With 360° torsion, mean initial rotation was 201° (range: 3.3–321.4°) and mean rotation after 24 h 215.7° (range 31.9–334.7°), respectively.
Conclusion: Direct postoperative imaging may not be accurate for determining the rotation of dDBS electrodes if a torque is present.

References

1. Reinacher PC, et al. Determining the Orientation of Directional Deep Brain Stimulation Electrodes Using 3D Rotational Fluoroscopy. AJNR

[7] MR-Based Proton-Density Fat Fraction (PDFF) Differentiates Between Patients with and Without Osteoporotic Vertebral Fractures and Between Osteoporotic and Traumatic Vertebral Fractures

Florian T. Gassert[1], Alexander Kufner[1], Felix G. Gassert[1], Yannik Leonhardt[1], Sophia Kronthaler[1], Benedikt J. Schwaiger[1,2], Christof Böhm[1], Marcus R. Makowski[1], Jan S. Kirschke[2], Thomas Baum[2], Dimitrios C. Karampinos[1], Alexandra S. Gersing[1]

[1]Department of Radiology, Klinikum Rechts der Isar, School of Medicine, Technical University of Munich, Munich, Germany
[2]Department of Neuroradiology, Klinikum Rechts der Isar, School of Medicine, Technical University of Munich, Munich, Germany

Purpose: To evaluate whether magnetic resonance (MR) imaging-based bone marrow Proton-Density Fat Fraction (PDFF) can differentiate between patients with and without acute osteoporotic/osteopenic vertebral fractures and whether PDFF values can differentiate between low-energy osteoporotic/osteopenic and high-energy traumatic vertebral fractures.
Methods: Of 52 study participants, 25 presented with one or multiple acute low-energy osteoporotic/osteopenic vertebral fractures of the lumbar spine (BMD<120 g/cm^3) and 7 patients with acute high-energy traumatic vertebral fractures (BMD>120 g/cm3). These patients were frequency-matched for age and sex to subjects without vertebral fractures ($N=20$). Bone mineral density (BMD) values were derived from quantitative CT. Chemical shift encoding-based water-fat MR imaging of the lumbar spine was performed considering a single T2* decay and PDFF maps were calculated. Segmentations of the vertebral bodies were performed excluding fractured vertebrae. Associations between category/fracture status and PDFF were assessed using multivariable linear regression models.
Results: A significant correlation between mean PDFF and BMD (r=–0.664, $P<0.001$) was found. In the osteoporotic/osteopenic group, those patients with osteoporotic/osteopenic fractures had a significantly higher PDFF than those without osteoporotic fractures after adjusting for age, sex and BMD (adjusted mean difference [95 % confidence interval]: 19.87 % [13.23 %, 26.50 %]; $P<0.001$). When evaluating all patients with acute vertebral fractures, those with high-energy traumatic fractures had a significantly lower mean PDFF than those with low-energy osteoporotic/osteopenic vertebral fractures ($P<0.001$).
Conclusion: MR-based PDFF enables the differentiation between patients with and without osteoporotic/osteopenic vertebral fractures as well as between low-energy osteoporotic/osteopenic and high-energy traumatic vertebral fractures, suggesting its potential as a biomarker for bone fragility.

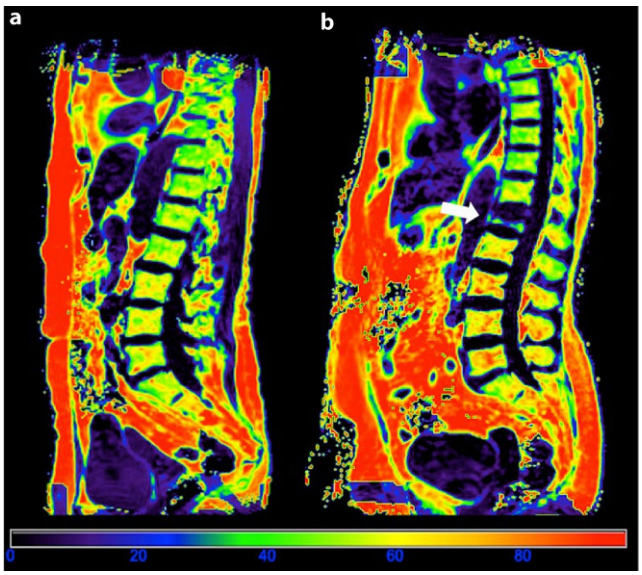

Fig. 1 Proton density fat fraction (PDFF) map [%] of an 80-year old female patient (a) without vertebral fracture and a low PDFF in the lumbar region (green and yellow regions) (a). PDFF map of a 73-year old female patient (b) with an osteoporotic vertebral fracture (arrow) in L! as well as a high PDFF in the lumbar regions (red and orange regions)

[8] Gray White Matter Blurring of the Temporal Pole Associated with Hippocampal Sclerosis: Analysis with T1 Mapping and Diffusion Mesoscopic Imaging

T. Demerath[1], M. Reisert[2,3], P. Reinacher[3], A. Rau[1], H. Urbach[1]

[1]Dept. of Neuroradiology, University Medical Center Freiburg
[2]Dept. of Medical Physics, University Medical Center Freiburg
[3]Dept. of Stereotactic and Functional Neurosurgery, University Medical Center Freiburg

Background & Purpose: On MRI, hippocampal sclerosis (HS) is often associated with gray/white matter blurring (GMB) of the temporal pole. In order to evaluate the microstructural substrate of GMB we acquired a MRI protocol including diffusion mesoscopic imaging and MP2RAGE sequences.
Methods: 13 patients with temporal lobe epilepsy and histologically proven hippocampal sclerosis were studied. Standardized temporal pole white-matter regions were segmented and diffusion measures and T1 relaxation times were compared in temporal poles ipsilateral to HS to values obtained from contralateral temporal poles and normal controls.
Results: Temporal poles on the HS side showed higher T1 values, lower white-matter intraaxonal volumes, lower fractional anisotropy and higher extraaxonal diffusivities compared to the contralateral temporal poles and normal controls. Changes were less pronounced in patients without visually obvious GMB but clearly different from the contralateral side and normal controls (Fig. 1).
Conclusion: Hippocampal sclerosis is associated with axonal loss of the ipsilateral temporal pole, even in patients in which these changes are not visible on FLAIR or T2-weighted sequences.

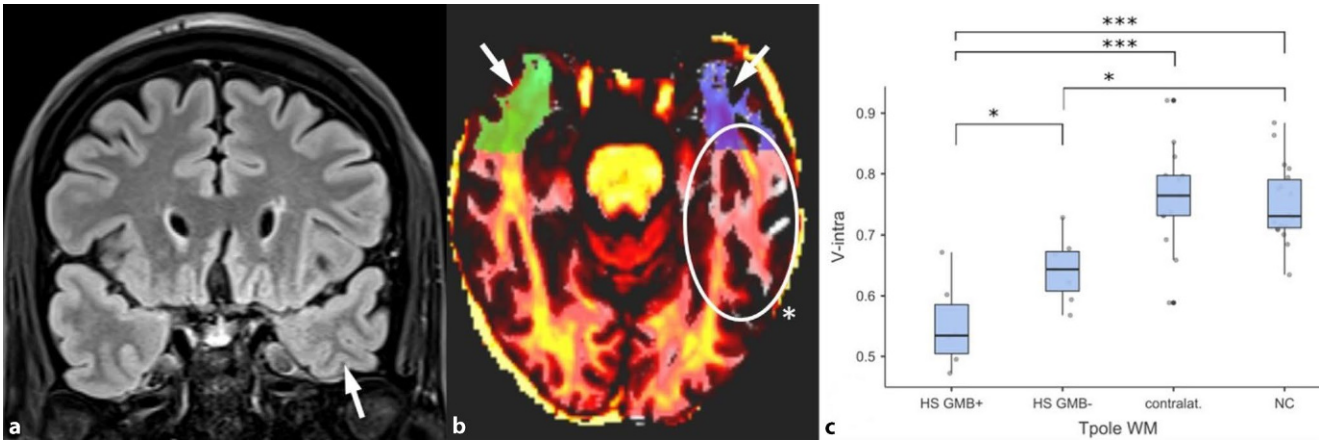

Fig. 1 Presurgical (3T) MRI in a patient with left-sided hippocampal sclerosis. Coronal FLAIR MRI shows left temporal lobe atrophy and subtle blurring of the temporopolar white matter (**a**, *arrow*). Axial fusion images combining white-matter segmentation and intraaxonal volume (V-intra) maps demonstrate V-intra loss extending far beyond the temporal pole (**b**, *). Changes are most pronounced in patients with FLAIR-visible GMB (HCS GMB+), but also present in patients without GMB (HCS-GMB-) when compared to the contralateral side and normal controls (**c**)

[9] Longitudinal 3D-FLAIR Substraction Maps: A Retrospective Single-Center Study

M. Mirkoei[1], H. Urbach[1], E. Kellner[2], T. Demerath[1]

[1]Dept. of Neuroradiology, University Medical Center Freiburg
[2]Dept. of Medical Physics, University Medical Center Freiburg

Background & Purpose: Longitudinal subtraction maps improve the detection of new lesions in MS follow-up. Nevertheless, current clinical applications for longitudinal FLAIR subtraction are not widespread and there is little data on subtraction imaging at 1.5 T. We tested a novel in-house developed longitudinal subtraction application and compared findings on 3D FLAIR subtraction maps with the clinical reports.

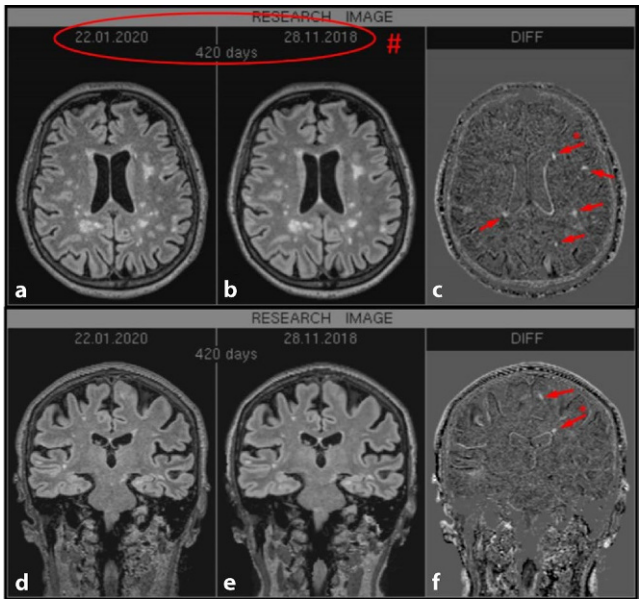

Fig. 1 NORA-based image output of longitudinal 3D-FLAIR (**a, b** axial; **d, e** coronal) and subtraction images (**c** axial; **f** coronal) in a patient with MS. One new T2-lesion in the left frontal deep white matter was initially missed on routine imaging without subtraction maps (**c, f** *arrow**). Four other new/growing lesions are also easily depictable on subtraction images (**c, f** *arrows*). The examination interval is easily readable in the output images (#)

Methods: Out of 95 follow-up examinations performed between 2016 and 2019, 33 cases (22 women; 18–56 years; 24 PRMS, four atypical MS, two MS in adolescence, one CIS, one suspected chronic inflammatory demyelinating disease, one RIS) were randomly included. 3D-FLAIR sequences were acquired at 1.5 T (Siemens Avanto) and 3 T MRI (Siemens Trio and Prisma). Subtraction maps were calculated using a NORA-based platform (www.nora-imaging.com), synchronized with the FLAIR 3D data sets and analyzed in a consensus reading (Fig. 1). New and larger lesions were annotated. Results were compared with the original reports.

Results: Using subtraction maps, discrepancies with previous reports were found in 14/33 patients: 6/33 had falsely been described as stable and new lesions were found in all cases. Larger lesions were found in 2/6 cases. In 8/33 cases new lesions were found in addition to new lesions described. In 7/8 of these cases, enlargement of lesions had not been described.

Conclusion: Congruently to others our study indicates that longitudinal 3D-FLAIR subtraction improves detection of new and growing lesions, even in 1.5 T MRI. Longitudinal 3D-FLAIR subtraction within a postprocessing pipeline constitutes a simple and effective tool for MS follow-up.

[10] Lower Lactate Levels and Lower Intracellular pH in IDH Mutant Versus Wildtype Glioma Patients

Katharina J. Wenger[1,3], Joachim P. Steinbach[2,3], Oliver Bähr [2,3], Ulrich Pilatus [1,3], Elke Hattingen[1,3]

[1]Department of Neuroradiology, University Hospital Frankfurt, Frankfurt am Main, Germany
[2]Department of Neurooncology, University Hospital Frankfurt, Frankfurt am Main, Germany
[3]German Cancer Consortium (DKTK) partner Site Frankfurt am Main/Mainz, Germany and German Cancer Research Center (DKFZ), Heidelberg, Germany

Background and Purpose: Preclinical evidence points towards a metabolic reprogramming in isocitrate dehydrogenase mutated tumor cells with downregulation of the expression of genes that encode for glycolytic metabolism. We non-invasively investigated lactate and Cr

concentrations, as well as intracellular pH using $^{1}H/^{31}P$ MRS in a glioma patient cohort.
Materials and Methods: 30 prospectively enrolled, mostly untreated glioma patients met the spectral quality criteria (WHO °II $n=7$, °III $n=16$, °IV $n=7$; IDHmut $n=23$, IDHwt $n=7$; 1p/19q codeletion $n=9$). MRI protocol included 3D ^{31}P CSI and ^{1}H single voxel spectroscopy (PRESS at TE 30 ms and TE 97 ms with optimized echo spacing for detection of 2-hydroxyglutarate) from the tumor area. Values for absolute metabolite concentrations were calculated (phantom replacement method). Intracellular pH was determined from ^{31}P CSI.
Results: At TE 97 ms, lactate peaks can be fitted with little impact of lipid/macromolecule contamination. We found a significant difference in lactate concentrations, lactate/Cr ratios, and intracellular pH comparing tumor voxels of IDHmut to IDHwt patients, with reduced lactate levels and near normal intracellular pH in IDHmut patients. We additionally found evidence for codependent effects of 1p/19q codeletion and IDH mutations with regard to lactate concentrations for tumor grades WHO °II and °III, with lower lactate levels in patients exhibiting the codeletion. There was no statistical significance comparing lactate concentrations between IDHmut WHO °II and °III gliomas.
Conclusion: We found indirect evidence for metabolic reprogramming in IDHmut tumors with significantly lower lactate concentrations compared to IDHwt tumors and a near normal intracellular pH.

[15] Neuroimaging Findings in Conjunction with Severe COVID-19 Infection

Büttner L[2], Bauknecht HC[1], Fleckenstein F[2], Kahn J[2], Tietze A[1], Bohner G[1], Siebert E[1]

[1]Department of Neuroradiology, Charité–Universitätsmedizin Berlin, Charitéplatz 1, 10117 Berlin, Germany
[2]Department of Radiology, Charité–Universitätsmedizin Berlin, Charitéplatz 1, 10117 Berlin, Germany

Background & Purpose: COVID-19 has a variable, but well–described course. Some patients additionally present with neurological symptoms. Recent studies also suggest neurological complications such as encephalitis. The purpose of this study was to investigate whether neuroimaging findings can be detected on CT and MRI in SARS-CoV-2 positive patients and whether they are direct sequelae of viral central nervous system infection or secondary to critical illness and intensive care therapy.
Methods: We retrospectively analyzed brain CT and MRI scans of 34 hospitalized COVID-19 patients at our Level I Center between March 15 and April 24 with regard to pathological neuroimaging findings. In addition, clinical parameters such as neurological symptoms, comorbidities, and type of ventilation therapy were documented. A descriptive statistical analysis was performed.
Results: Pathological findings were detected in 38.2 % of patients of the study cohort. Based on the weekly institutional SARS-CoV-2 report of all positively tested patients in our clinic at the time of data collection, neuroimaging findings could be found in 6 % of all patients (34/565). The most common findings were microbleeds (20.6 %) and signs of hypoxic brain injury (11.8 %). Furthermore, cortical subarachnoid hemorrhage, typical and atypical cerebral hematomas, ischemic strokes, and generalized brain edema were documented. All neuroimaging findings occurred in patients who were either intubated or treated by ECMO.
Conclusion: A broad range of pathological neuroimaging findings can be seen in critically ill SARS-CoV-2 positive patients. The majority of neuroimaging findings are probably critical illness and therapy-associated, although direct and indirect viral effects cannot be excluded.

[20] Smoking is a Major Contributor of Peripheral Nerve Damage in Diabetic Polyneuropathy

Mooshage CM[1], Jende JME[1], Kender Z[2], Heiland S[1], Nawroth PP[2], Bendszus M[1], Kopf S[2], Kurz FT[1]

[1]Department of Neuroradiology, Heidelberg University Hospital
[2]Department of Endocrinology, Diabetology and Clincal Chemistry (Internal Medicine 1), Heidelberg University Hospital

Background & Purpose: So far it remains unclear whether smoking-induced microangiopathic changes contribute to the damage of peripheral nerves in diabetic polyneuropathy (DPN). The aim of this study was to investigate the correlation between cigarette smoking and peripheral nerve damage in diabetic polyneuropathy.
Methods: We performed 3 T MR-neurography of the right leg in 77 patients (34 never smokers, 32 ex-smokers, 11 active smokers; female: 32, male: 35). Semi-automated analysis of lesion load and nerve average diameter was performed. In addition, clinical, serological and electrophysiologic parameters were assessed.
Results: A significantly higher load of T2w-hyperintense sciatic nerve lesions were found in smokers compared to ex-smokers (20.8 % ±7.2 vs. 9.%±1.1 respectively 7.4 % ± 0.9, respectively $p<0.001$). Also, we identified a significantly larger diameter of sciatic nerve in smokers (162 $mm^2 \pm 18$) in comparison to ex-smokers (130.2 $mm^2 \pm 5$) and to never smokers (127 $mm^2 \pm 5$; $p=0.024$). Lesion load and diameter of sciatic nerve also showed a negative correlation between peroneal nerve conduction velocity ($r=-0.29$; $p=0.008$ respectively $r=-0.28$; $p=0.012$) and Neuropathy Disability Score ($r=0.32$; und $r=0.33$; respectively $p<0.001$). We did not find a correlation for HbA1c-values.
Conclusion: Our results reveal a significant association of smoking on peripheral nerve damage in diabetic neuropathy. Both peripheral nerve diameter and increased lesion load of sciatic nerve are further associated with a lower nerval conduction velocity.

[22] Decreased Amygdala Nuclei Volumes in Adulthood After Premature Birth

Schmitz-Koep B, MD[1,2]; Bäuml J G, PhD[1,2]; Menegaux A, PhD[1,2]; Nuttall R, MSc[1,2]; Zimmermann J, MSc[1,2]; Schneider S C, BSc[1,2]; Daamen M, PhD[3,4]; Boecker H, MD[3]; Zimmer C, MD[2]; Wolke D, PhD[5,6]; Bartmann P, MD[4]; Sorg C, MD[1,2,7]; Hedderich D M, MD, MHBA[1,2]

[1]Department of Neuroradiology, School of Medicine, Technical University of Munich, Ismaninger Str. 22, 81675 Munich, Germany
[2]TUM-NIC Neuroimaging Center, School of Medicine, Technical University of Munich, Ismaninger Str. 22, 81675 Munich, Germany
[3]Functional Neuroimaging Group, Department of Radiology, University Hospital Bonn, Venusberg-Campus 1, Bonn, Germany
[4]Department of Neonatology, University Hospital Bonn, Venusberg-Campus 1, Bonn, Germany
[5]Department of Psychology, University of Warwick, University Road, Coventry, CV4 7AL, United Kingdom
[6]Warwick Medical School, University of Warwick, University Road, Coventry, CV4 7AL, United Kingdom
[7]Department of Psychiatry, School of Medicine, Technical University of Munich, Ismaninger Str. 22, 81675 Munich, Germany

The amygdala is located in the medial temporal lobe and is composed of several grey matter nuclei that are divided into centromedial, basolateral and superficial nuclei based on their distinct ontogeny and developmental trajectories[1]. While previous studies reported lower whole amygdala volumes after premature birth[2,3,4], the effect of premature birth on amygdala subnuclei remains unknown.

We hypothesized differential effects of premature birth on centromedial and basolateral amygdala. We addressed this question by state-of-the-art amygdala subnuclei segmentation using Freesurfer in a large

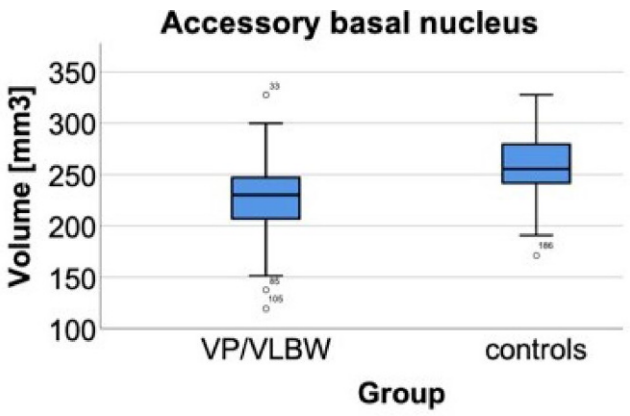

Fig. 1 Group comparison of accessory basal nucleus volumes in premature-born individuals compared to controls. These Boxplots show mean bilateral volumes of the accessory basal nucleus in individuals born very preterm and/or with very low birth weight (VP/VLBW) ans in full-term controls. Marginal means as estimated by the general linear model with left or right whole amygdala volume, respectively, sex and scanner as covariates were significantly smaller in premature-born individuals compared to controls (left 239.5 mm^3 vs. 244.5 mm^3, $p=0.003$; right: 241.2 mm^3 vs. 246.7 mm^3, $p=0.003$)

and prospectively collected cohort of 101 very premature-born adults (<32 weeks of gestation and/or birth weight below 1500 g) and 108 full-term controls at 26 years of age.

We found significantly lower whole amygdala volumes in premature-born adults. Also, amygdala composition differed in premature-born adults, which showed significantly lower volumes of the accessory basal nucleus (pertaining to the basolateral amygdala), adjusted for whole amygdala volume. Moreover, association with variables of premature birth (gestational age, birth weight and duration of ventilation) was moderate for basolateral and superficial amygdala nuclei and absent for left centromedial amygdala nuclei.

Our data suggests differentially affected development of the basolateral amygdala after premature birth, possibly through disturbance of distinct developmental pathways.

References

1. Swanson, L.W., & Petrovich, G.D. (1998). What is the amygdala? Trends in Neurosciences.
2. Peterson, B.S. et al. (2000). Regional brain volume abnormalities and long-term cognitive outcome in preterm infants. Journal of the American Medical Association.
3. Cismaru, A.L. et al. (2016). Altered Amygdala Development and Fear Processing in Prematurely Born Infants. Frontiers in Neuroanatomy.
4. Walker, S.M. et al. (2018). Somatosensory function and pain in extremely preterm young adults from the UK EPICure cohort: sex-dependent differences and impact of neonatal surgery. British Journal of Anaesthesia.

[23] AI-Guided Pathology Detection in Routine Head CT

Finck T[1], Schinz D[1], Zimmer C[1], Pfister F[2], Wiestler B[1]

[1]Abteilung für Diagnostische und Interventionelle Neuroradiologie, Klinikum rechts der Isar der Technischen Universität München
[2]deepc GmbH

Background & Purpose: Computed tomography (CT) continues to be the workhorse in neuroradiology with an ability to detect a wide variety of intracranial pathologies in a highly timely manner. Recent advances in machine-learning allow for the question how an Artificial Intelligence tool can detect abnormalities on head CT and support the radiologist.

Methods: We evaluated a novel machine learning tool (*Deepc*) to automatically detect intracranial pathologies and provide patient-level predictions on the lack/presence of pathological findings, as well as a voxel-level heatmap, highlighting pathologies

Results: Of the 447 CT scans that were acquired during the study period (March 2020), 247 were eligible for inclusion after filtering for multiple scans/patient ($n=159$), implanted metal devices ($n=40$) and processing errors ($n=1$). In these, *Deepc* provided definite ratings (into healthy/pathological) in 166 patients and indeterminate ratings (i.e. not reaching a threshold for definite labellings) in 81 patients. Accuracy to predict the lack/presence of any pathology was 98 % (Senstivity 100 %, Specificity 86 %) in a collective-wide evaluation comprising unselected patients with strokes of different stages, SAH, SDH, ICB, as well as intracranial masses, to only cite the most common pathologies. Of note, no pathological head CT was wrongfully labelled as ''healthy'' by the machine-learning tool.

Conclusion: AI-guided pathology detection in head CT is feasible in an unselected collective mirroring the routine clinical workflow. While a margin of uncertainty remains in giving definite ratings, no patient with intracranial pathology was wrongfully labelled as ''healthy'' in a collective of 247 subjects. Future work on continuous learning of such systems might help to further increase its use.

[33] DCE-MRI Assessment of Blood-Brain Barrier Permeability in Early Alzheimer's Disease

Villringer K[1], Preis L[3], Cetindag A[2], Peters O[2,3], Fiebach JB[1]

[1]Center for Stroke Research Berlin, Charité–Universitätsmedizin, Berlin
[2]Department of Psychiatry and Psychology, Campus Benjamin Franklin, Charité–Universitätsmedizin, Berlin
[3]German Center for Neurodegenerative Diseases, Berlin

Background and Purpose: Recently, it could be demonstrated that the disruption of the blood-brain barrier (BBB) in the hippocampus correlates with functional cognitive impairment[1] independent of Alzheimer's disease (AD) pathology. Aim of this study was to assess the BBB in the AD continuum.

Method: Examination on a 3 T MR scanner (Prisma_fit, Siemens AG). The dynamic contrast enhanced (DCE) protocol comprised pre-contrast T1 measurements with 4 different flip angles (2°, 10°, 20°, 35°) for T1 mapping, as well as continuous serial acquisitions of 60 volumes after administration of 10 ml contrast agent at a flow rate of 1 ml/s. Patlak analysis was employed to assess BBB permeability using the open source software package ROCKETSHIP (https://github.com/petmri/ROCKETSHIP). Study participants were characterized according to the clinical dementia rating (CDR) and categorized as normal controls (NC) and cognitive impairment due to AD.

Results: We examined 81 participants (MCI+ $n=29$, NC=52). Mean age was 74.4±6.5 years, 33 (40.7 %) were females. The median MMSE for MCI+ was 25, for NC 29. Median Wahlund score[2] for MCI was 6, for NC 4.

After controlling for age, Wahlund score, vascular risk factors and log transformation of mean K^{trans} values, participants with cognitive impairment as defined by the CDR in combination with neuropsychological deficits showed a disruption of the hippocampal BBB (left $p=0.04$, right $p=0.035$). An example of a bilateral BBB permeability disruption is given in Fig. 1.

Conclusion: Using DCE-MRI early BBB disruption can be detected in the AD continuum independently of vascular risk factors and white matter lesions.

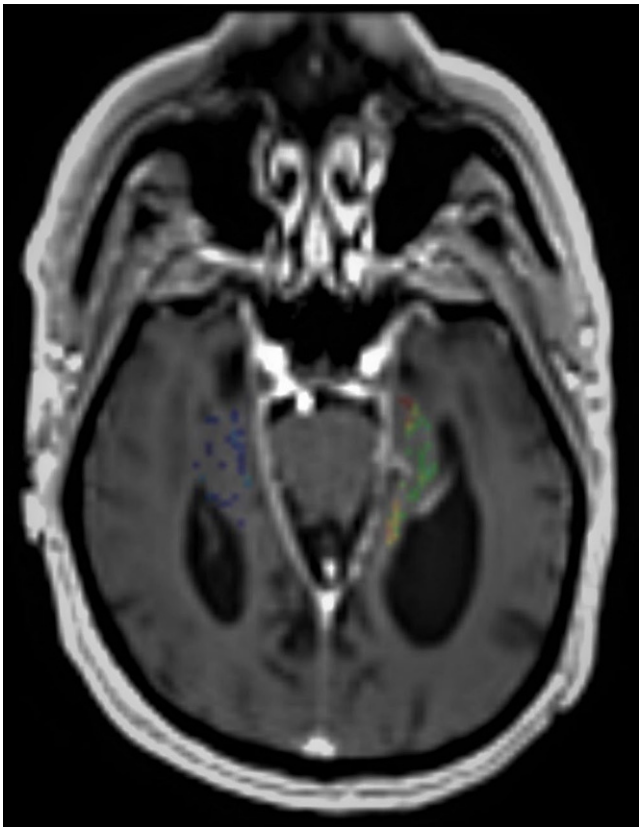

Fig. 1

References

1. Nation DA et al., Blood-brain barrier breakdown is an early biomarker of human cognitive dysfunction. Nat Med 2019;25:270–276
2. Wahl und LO et al. A new scale for age-related white matter changes applicable to MRI and CT. Stroke 2001;32:1318–1322

[41] Accuracy and Reliability of PBV-ASPECTS, CBV-ASPECTS and NECT-ASPECTS in Acute Ischemic Stroke: A Matched-Pair Analysis

Falbesaner A, Pfaff JAR, Seker F, Heiland S, Bendszus M, Potreck A

Department of Neuroradiology, Heidelberg University Hospital, Germany

Purpose: To investigate the reliability and accuracy of Alberta Stroke Program Early CT Scores (ASPECTS) derived from flat-panel-CT-perfusion parenchymal-blood-volume-(PBV)- maps compared to conventional CT-Perfusion CBV-maps and non-enhanced CT (NECT).
Methods: ASPECTS from flat-panel derived PBV-maps were evaluated retrospectively by two experienced readers for 37 consecutive patients with acute MCA M1-occlusion who underwent flat-panel-CT-perfusion imaging before mechanical thrombectomy between 11/2016 and 02/2019. For comparison with ASPECTS from conventional NECT and from CT-perfusion derived CBV-maps, a matched-pair analysis according to pre-stroke mRS, age, stroke severity, site of occlusion, time from stroke onset to admission and final TICI was performed with patients who underwent NECT and Perfusion-CT prior to mechanical thrombectomy between 6/2015 and 2/2019. Follow-up ASPECTS was derived for all patients from either conventional NECT or (in $n=7$ patients) from MRI (FLAIR) 24 h after mechanical thrombectomy. In cases of disagreement, consensus rating was reached.
Results: Interrater-agreement was only moderate for PBV-ASPECTS (w-Kappa = 0.53), while it was substantial for CBV-ASPECTS (w-Kappa = 0.63) and best for NECT-ASPECTS (w-Kappa = 0.74). Accuracy, as assessed by spearman correlation between acute and follow-up ASPECTS in patients with successful recanalization (mTICI 2b or better), was best for NECT-ASPECTS (rho = 0.86 (0.65–0.97), $p<0.001$), while it was comparable for PBV-ASPECTS (rho = 0.55 (0.24–0.81), $p=0.01$) and CBV-ASPECTS (rho = 0.56 (0.18–0.85), $p<0.001$). Noteworthy, cases of relevant infarct overestimation occurred in both acute PBV- and CBV-ASPECTS evaluation.
Conclusion: NECT-ASPECTS prior to mechanical thrombectomy outperformed both PBV-ASPECTS and CBV-ASPECTS in accuracy and reliability, while the latter two were found to be comparable in accuracy but not in reliability.

[42] Accelerating Multiple Sclerosis Imaging with Attention to Detail

Hongwei Li[1,2], Timo Löhr[1,2], Tom Finck[1], Claus Zimmer[1], Mark Mühlau[3], Björn Menze[2], Benedikt Wiestler*[2]

[1]Dept. of Neuroradiology, TU Munich University Hospital, Munich, Germany
[2]Dept. of Informatics, TU Munich, Munich, Germany
[3]Dept. of Neurology, TU Munich University Hospital, Munich, Germany

Background & Purpose: Advances in image acquisition [1] and Deep Learning-based image synthesis [2] synergistically accelerate high-resolution MR imaging of Multiple Sclerosis (MS) patients. Here, we present preliminary results on a novel, lesion-attention GAN (Generative Adversarial Network) for full-resolution image synthesis with a special attention on (small) lesion translation, allowing a full examination (T1w, T2w, FLAIR, DIR, all 3D 1 mm isotropic) in less than seven minutes.
Methods: To refine our DiamondGAN architecture [3] with special emphasis on the reliable reconstruction of (small) MS lesions, we added an additional L1 loss based on automatically created lesion segmentation maps for the cycle-consistency loss. This network was trained on 30 subjects to generate FLAIR and DIR sequences from input T1w and T2w (both acquired with compressed sensing in 1 mm isotropic resolution in less than seven minutes). For comparison, we also trained a standard CycleGAN without lesion attention.
Results: Median Contrast-Noise-Ratio (CNR) for MS lesions was comparable between acquired and synthetic (AttentionGAN, CycleGAN) DIR images (27.3 vs. 24.2 vs. 20.5), while CNR was lower for synthetic FLAIR images (12.9 vs. 10.3 vs. 9.7). However, in particular small lesions were visually better translated in AttentionGAN (Fig. 1).
Conclusion: Combining compressed sensing and image synthesis potentially allows to acquire a full MS MR examination with 3D 1 mm isotropic sequences in less than seven minutes by synthesizing DIR and FLAIR contrasts from T1w and T2w sequences. Future work will focus on optimizing the loss term for balancing lesion translation and halluzination.

References

1. Eichinger et al., Acceleration of Double Inversion Recovery Sequences in Multiple Sclerosis With Compressed Sensing. Investigative Radiology (2019)
2. Finck et al., Deep-Learning Generated Synthetic Double Inversion Recovery Images Improve Multiple Sclerosis Lesion Detection. Investigative Radiology (2020)
3. Li et al., DiamondGAN: Unified Multi-Modal Generative Adversarial Networks for MRI Sequences Synthesis. MICCAI (2019)

Fig. 1

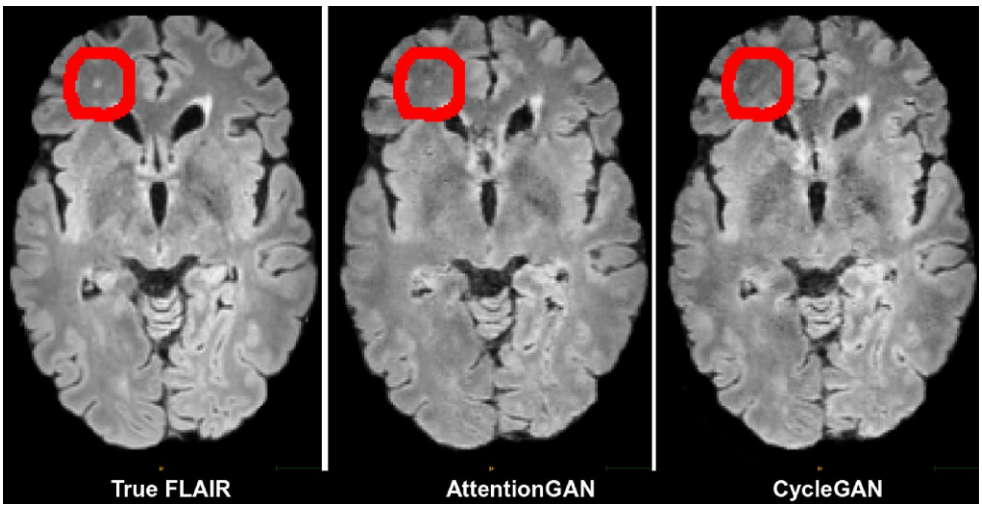

[47] Local Cellular Inflammatory Responses During Hyperacute Human Ischemic Stroke are Robust and Reproducible

Alexander M. Kollikowski, MD[1]; Michael K. Schuhmann, PhD[2]; Bernhard Nieswandt, PhD[3]; Wolfgang Müllges, MD[2]; Guido Stoll, MD[2]; Mirko Pham, MD[1]

[1]Departments of Neuroradiology, University Hospital of Würzburg, Würzburg, Germany
[2]Departments of Neurology, University Hospital of Würzburg, Würzburg, Germany
[3]Institute of Experimental Biomedicine, University Hospital and Rudolf Virchow Center, University of Würzburg, Würzburg, Germany

Background and Purpose: Probing the arterial compartment during the hyperacute stage of vascular occlusion is crucial to establish the relevance of local inflammation in human ischemic stroke and to overcome translational barriers impeding the implementation of adjunct treatment strategies beyond recanalization.[1,2]
Methods: We have recently described a protocol to obtain matched local ischemic (distal/D) and systemic (carotid (C) and femoral (F)) arterial blood sample triplicates in stroke patients with embolic large vessel occlusion of the anterior circulation who underwent mechanical thrombectomy.[3] Applying this protocol, we prospectively observed 304 consecutive patients in all of whom blood sampling was attempted. Light microscopy of Pappenheim-stained smears was applied for white blood cell differential and platelet counting.
Results: White blood cell differential and platelet counting was performed in seventy-one patients who met all clinical, imaging, interventional, and laboratory inclusion criteria. We observed a selective increase in leukocyte counts within the ischemic arterial compartment, which was mainly determined by neutrophil accumulation (D vs C: +9.8 %; D vs F: +16 %; $p<0.0001$). Consistently, a significant local increase was found for the lymphocyte subpopulation (D vs F: +11.8 %; $p=0.0117$). No significant variations were seen for monocytes. Finally, we observed a significant local decrease in platelet counts (D vs F: –4.5 %; $p=0.0387$).
Conclusion: We confirm the previously reported finding of a locally selective leukocyte accumulation during hyperacute human ischemic stroke and present first data on concurrent luminal platelet consumption. These data indicate that local platelet/leukocyte interactions may already be operative under the occlusion condition.

Funded by the German Research Foundation (374031971-TRR 240)

References

1. Sommer CJ. Ischemic stroke: experimental models and reality. *Acta Neuropathol*. 2017;133(2):245–261. https://doi.org/10.1007/s00401-017-1667-0
2. Stoll G, Nieswandt B. Thrombo-inflammation in acute ischaemic stroke–implications for treatment. *Nat Rev Neurol*. July 2019. https://doi.org/10.1038/s41582-019-0221-1
3. Kollikowski AM, Schuhmann MK, Nieswandt B, Müllges W, Stoll G, Pham M. Local Leukocyte Invasion during Hyperacute Human Ischemic Stroke. *Ann Neurol*. 2020;87(3):466–479. https://doi.org/10.1002/ana.25665

[51] Multimodal Validation of Focal Enhancement in Intracranial Aneurysms as an Imaging Marker of a Higher Risk of Rupture

Larsen N[1], Saalfeld S[2,3], Flüh C[4], Voß S[2,5], Hille G[2,3], Pravdivtseva M[1], Berg P[5]

[1]Department of Radiology and Neuroradiology, University Hospital Schleswig-Holstein, Campus Kiel, Kiel, Germany
[2]Forschungscampus *STIMULATE*, University of Magdeburg, Magdeburg, Germany
[3]Department of Simulation and Graphics, University of Magdeburg, Magdeburg, Germany
[4]Department of Neurosurgery, University Hospital Schleswig-Holstein, Campus Kiel, Kiel, Germany
[5]Laboratory of Fluid Dynamics and Technical Flows, University of Magdeburg, Magdeburg, Germany

Background and Purpose: Focal enhancement on MR vessel wall imaging is frequently encountered in unruptured intracranial aneurysms, but its implication for risk stratification and patient management remains unclear. This study investigates the association of focal wall enhancement with established clinical, hemodynamic and morphological risk factors and histologic markers of wall degradation.
Methods: Patients with an unruptured middle cerebral artery aneurysm who underwent 3 T MR vessel wall imaging and 3D rotational angiography (RA) were included. Segmentations of enhanced MR areas and the 3D aneurysm model based on RA were carried out and co-registered.

Hemodynamic parameters were calculated based on flow simulations and compared between enhanced regions and the entire aneurysm surface. Morphological parameters were semi-automatically extracted and quantitatively associated with wall enhancement. Histological

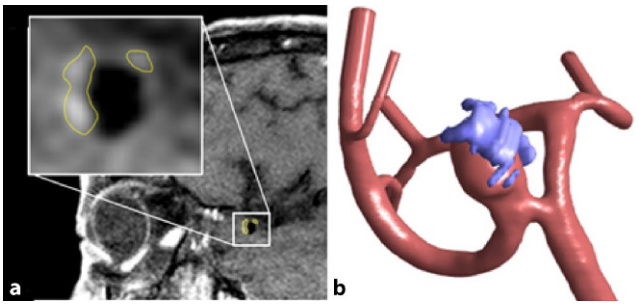

Fig. 1 Manual segmentation of enhanced areas on black blood MRI (**a**) and registration with the aneurysm surface (**b**)

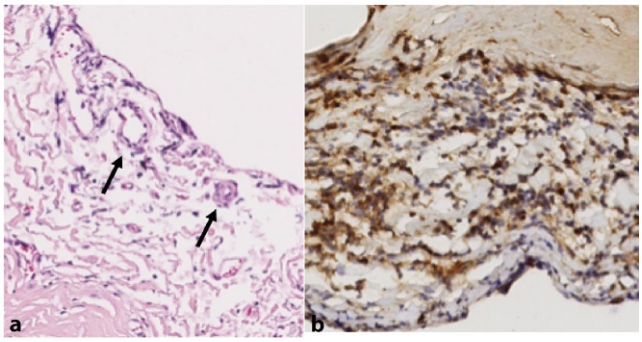

Fig. 2 **a** Hematoxylin and eosin stain depicting adventitial vasa vasorum (*arrows*). **b** Myeloperoxidase (MPO) stain demonstrating MPO-positive inflammatory cell invasion in brown

analysis included detection of vasa vasorum, CD34 and myeloperoxidase staining in a subset of patients.
Results: Twenty-two aneurysms were analyzed. Enhanced regions were significantly associated with lower cycle-averaged wall shear stress, lower maximum oscillatory shear, and increased low shear area. Higher PHASES score and histological signs of wall inflammation and degeneration were significantly associated with focal enhancement. Higher ellipticity index was an independent predictor of wall enhancement.
Conclusion: Focal wall enhancement is co-localized with hemodynamic factors that have been related to a higher rupture risk. It is correlated with morphological factors linked to a higher rupture risk, higher PHASES scores and histologic markers of wall destabilization. The results support the hypothesis that focal enhancement could serve as a surrogate marker for a higher risk of rupture.

[56] Repeated Mechanical Thrombectomy in Short-Term Large Vessel Occlusion Recurrence: Multicenter Study and Systematic Review of Literature

Hanna Styczen[1], Christian Maegerlein[2], Leonard Yeo[3], Christin Clajus[4], Andreas Kastrup[5], Nuran Abdullayev[6], Daniel Behme[7], Christoph J. Maurer[8], Lukas Meyer[9], Lukas Goertz[10], Benno Ikenberg[11], Benjamin Yong-Qiang Tan[3], Donald Lobsien[4], Panagiotis Papanagiotou[12], Christoph Kabbasch[6], Amélie Carolina Hesse[7], Ansgar Berlis[8], Jens Fiehler[9], Sebastian Fischer[13], Michael Forsting[1], Volker Maus[13]

[1]Institute for Diagnostic and Interventional Radiology and Neuroradiology, University Hospital Essen, Essen, Germany
[2]Department of Diagnostic and Interventional Neuroradiology, Klinikum rechts der Isar, Technical University Munich, Munich, Germany
[3]Division of Neurology, Department of Medicine, National University Health System, Singapore
[4]Department of Diagnostic and Interventional Radiology and Neuroradiology, Helios General Hospital Erfurt, Erfurt, Germany
[5]Department of Neurology, Klinikum Bremen, Bremen, Germany
[6]Department of Diagnostic and Interventional Radiology, University Hospital Cologne, Cologne, Germany
[7]Institute for Diagnostic and Interventional Neuroradiology, University Hospital Goettingen, Goettingen, Germany
[8]Department of Diagnostic and Interventional Neuroradiology, University Hospital Augsburg, Augsburg, Germany
[9]Department of Diagnostic and Interventional Neuroradiology, University Medical Center Hamburg-Eppendorf, Hamburg, Germany
[10]Center for Neurosurgery, Medical Faculty and University Hospital, University of Cologne, Cologne, Germany
[11]Department of Neurology, Klinikum rechts der Isar, Technical University Munich, Munich, Germany
[12]Department of Neuroradiology, Hospital Bremen-Mitte & National and Kapodistrian University of Athens, Greece
[13]Department of Radiology, Neuroradiology and Nuclear Medicine, University Medical Center Langendreer, Bochum, Germany

Background: Data on the frequency and outcome of repeated mechanical thrombectomy (MT) in patients with short-term re-occlusion of intracranial vessels is limited. Addressing this subject, we report our multicenter experience with a systematic review of the literature.
Methods: A retrospective analysis was conducted of consecutive acute stroke patients treated with MT repeatedly within 30 days at 10 tertiary care centers between January 2007 and January 2020. Baseline demographics, etiology of stroke, angiographic outcome and clinical outcome evaluated by the modified Rankin Scale (mRS) at 90 days were noted. Additionally, a systematic review of reports with repeated MT due to large vessel occlusion (LVO) recurrence was performed.
Results: We identified 30 out of 7844 (0.4 %) patients who received two thrombectomy procedures within 30 days due to recurrent LVO. Through systematic review, three publications of 28 participants met the criteria for inclusion. Combined, a total of 58 participants were analyzed: cardioembolic events were the most common etiology for the first (65.5 %) and second LVO (60.3 %), respectively. Median baseline NIHSS (National Institutes of Health Stroke Scale) was 13 (IQR 8–16) before the first MT and 15 (IQR 11–19) before the second MT ($p=0.031$). Successful reperfusion was achieved in 91.4 % after the first MT and in 86.2 % patients after the second MT ($p=0.377$). The rate of functional independence (mRS 0–2) was 46 % at 90 days after the second procedure.
Conclusion: Repeated MT in short-term recurrent LVO is a rarity but appears to be safe and effective. The second thrombectomy should be pursued with the same extensive effort as the first procedure as these patients may achieve similar good outcomes.

[60] Pseudoprogression in Pediatric Low-Grade Glioma Following Primary Radiotherapy–Results from the German LGG Cohort

Annika Stock[1,2], Caroline V. Hancken[1,3], Daniela Kandels[4], Astrid K. Gnekow[4], Rolf-Dieter Kortmann[5], Stefan Dietzsch[5], Beate Timmermann[6], Torsten Pietsch[7], Mirko Pham[1], Brigitte Bison[1,2], Monika Warmuth-Metz[1,2]

[1]Department of Neuroradiology, University Hospital Wuerzburg, Wurzburg, Germany
[2]National Reference Center for Neuroradiology, Wuerzburg, Germany
[3]Department of Diagnostic and Interventional Radiology, Section of Pediatric Radiology, University Hospital Hamburg-Eppendorf, Hamburg, Germany
[4]Swabian Children's Cancer Center, University Hospital Augsburg, Augsburg, Germany
[5]Department of Radiation Oncology, University of Leipzig, Leipzig
[6]Department of Particle Therapy, University Hospital Essen, West German Proton Therapy Centre Essen (WPE), West German
[7]Cancer Centre (WTZ), German Cancer Consortium (DKTK), Germany
[8]Institute of Neuropathology, DGNN Brain Tumor Reference Center, University of Bonn Medical Center, Bonn, Germany

Background & Purpose: Expansion of MRI T2-weighted and/or T1-weighted lesion volume after radiotherapy (RT) may indicate pseudoprogression (PsPD). The differentiation between true progression and PsPD is a diagnostic and therapeutic challenge and it is underinvestigated particularly in pediatric low-grade glioma (LGG). The aim of this study was to apply radiological and clinical criteria for PsPD in pediatric LGG following three RT-modalities to estimate the incidence of PsPD.
Methods: 133 pediatric LGG patients (68 [51.1 %] male, median age at therapy start 11.36 years [range 0.78–25.92]) of the SIOP-LGG 2004 study and registry with primary RT (iodine-seed-brachytherapy [IS; $n=51$], photon-beam [PT; $n=60$] or proton-beam RT [PBRT; $n=22$]) were included. Initial and regular follow-up brain MRI over 2 years were evaluated. Increasing 1) total tumor-associated T2-lesion, 2) focal tumor-associated T2-lesion and 3) T1-weighted contrast-enhancing tumor were the evaluated items according to which PsPD suspicion was raised. Their imaging behavior over a follow-up of 2 years finally determined true PsPD.
Results: True PsPD was radiologically determined in 54/119 (45.4 %) and was not dependent on the RT-modality applied (IS 43.8 %; PT 47.2 %; PBRT 44.4 %; $p=0.939$). True PsPD occurred at a median of 6.1 months after RT initiation and persisted for a median of 7 months (IS 7.8 months; PT 6.25 months; PBRT 8.1 months). Finally, intratumoral necrosis within the focal tumor-associated T2-lesion predicted true progression ($p<0.001$).
Conclusion: PsPD in irradiated pediatric LGG is substantially frequent and seems not to depend on the modality of primary RT applied (IS vs. PT vs. PBRT).

[63] Neuroradiological Emergency Consultations During the Early Weeks of the COVID-19 Pandemic

Harlan M[1], Pfaff G[2], Bendszus M[1], Pfaff JAR[1]

[1]Department of Neuroradiology, Heidelberg, Germany
[2]Visiting Lecturer in Epidemiology and Psychiatric Epidemiology, Protestant University of Applied Sciences Ludwigsburg

Background & Purpose: Social distancing and stay-at-home advisories aimed at reducing COVID-19 spread may inadvertently affect emergency medical care. We analyzed the time course of neuroradiological emergency consultations (NECs) in a teleradiological network before and after implementation of COVID-19 pandemic lockdown measures.
Methods: We performed an ambispective observational study of NECs in a teleradiological network connecting a tertiary care university hospital and thirteen hospitals in Southwest Germany. The study period covered prepandemic calendar weeks (CW) 01/2019–11/2020, and COVID-19 pandemic weeks 12–28/2020. Descriptive data on NEC computed tomography imaging from the prepandemic period were compared with prospective observations for the pandemic period.
Results: During the prepandemic study period, the number of NECs per week remained stable around a median of 103 (interquartile range [IQR]: 97–115). After Germany entered COVID-19 lockdown in CW 12/2020, teleconsultations declined sharply, followed by a slow rebound (median: 80, IQR: 67–88; p-value <0.001). Following gradual loosening of the lockdown starting in CW 20/2020, the weekly number of NECs rose to exceed the comparison figures for 2019 (median: 111, IQR: 100–129; p-value: 0.13, see Fig. 1).
Conclusion: After the implementation of COVID-19 pandemic lockdown measures in Germany, we observed a temporary massive decline in neuroradiological emergency consultations. This depression may correspond to a period of delayed or missed opportunities for early diagnostic workup and treatment of neurological emergency situations. We recommend educating the public about both COVID-19 precautions and the overriding importance to seek immediate medical care in health emergencies such as stroke.

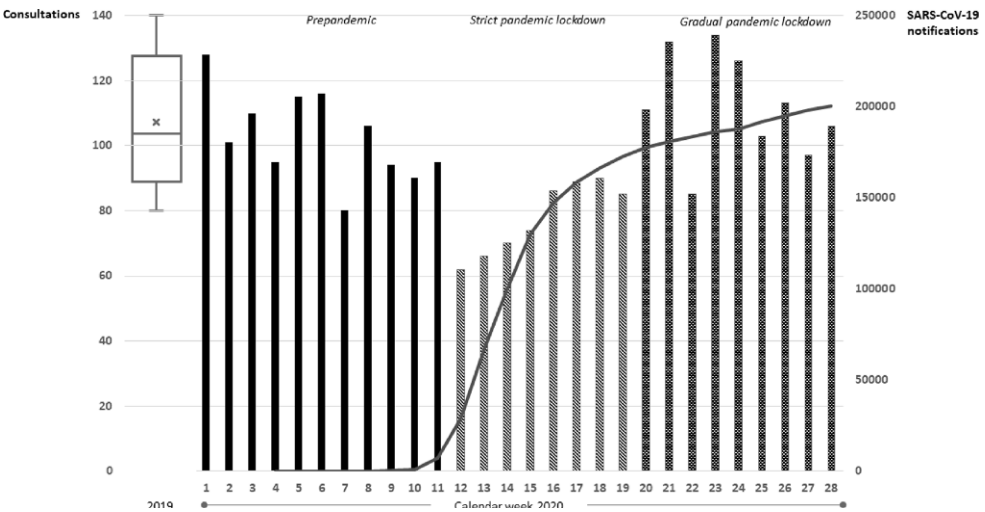

Fig. 1 Number of neuroradiological emergency consultations in a teleradiological network in the reference year 2019 (boxplot), and by calendar week (bars), and cumulative number of notified SARS-CoV-2 infections in Germany* (line) during pandemic lockdown phases in calendar weeks 01-28/2020. *Source: Johns Hopkins University Center for Systems Science and Engineering (CSSE)

[12] Retinal Diffusion Restrictions in Central Retinal Artery Occlusion: Time Course and Correlation with Clinical Features as well as Ophthalmoscopic Findings

Danyel L[1], Siebert E[2]

[1]Department of Neurology, Charité–Universitätsmedizin Berlin
[2]Institute of Neuroradiology, Charité–Universitätsmedizin Berlin

Background and Purpose: To systematically evaluate retinal diffusion restrictions (RDR) in patients with central retinal artery occlusion (CRAO) using a standard stroke DWI-EPI sequence.
Methods: Consecutive patients with CRAO between 01/2010 and 12/2019 and stroke-MRI performed within 2 weeks of clinical onset were included. Patient data, including visual acuities (VA), fundoscopic features, medical history, laboratory findings, and intravenous thrombolysis were recorded. DWI was evaluated for RDR by a neuroradiologist blinded for CRAO side and clinical data.
Results: 127 patients (mean age 69.6 ± 13.9; 59 female) were included. RDR were present in 67.2 % of patients overall and in 78.6 % within the first 24 h (arrows Fig.). Only in one case (0.8 %) was RDR falsely attributed to the wrong side. There was a trend for RDR to be more frequent in patients with blindness compared to less severe visual impairment ($p = 0.07$). Absence of RDR was more frequent in patients with complete VA restitution (75 %) vs. without remission (28.4 %; $p = 0.006$). Patients without retinal opacity or cherry red spot on ophthalmoscopy were more likely to show no RDR compared to those with these findings (60 % vs. 27.1 %; $p = 0.004$). Overall detection rates of RDR did not differ significantly within the first week, but dropped significantly in the second week (>7–14 d 10.0 %; $p = 0.0006$).
Conclusions: Retinal diffusion restrictions are present in a majority of CRAO patients and are time dependent. They tend to match clinical and ophthalmoscopic severity. Further work should explore the potential of stroke DWI in the hyperacute phase for patient selection for recanalizing therapies.

[44] Correlation of Clinical Diagnosis and Parameters with the Extent of the Endolymphatic Hydrops, Visualized by MRI

Grosser, D.[1], Willenborg, K[2]., Böthig, D[3]., Avalone, E[2]., Götz, F[1]., Warnecke, A[2]., Lanfermann, H[1]., Giesemann, A[1]

[1]Institute of Neuroradiology, Hannover Medical School
[2]Department of Otorhinolaryngology, Hannover Medical School
[3]Department of Pediatric Cardiology, Hannover Medical School

Background and Purpose: Visualization of the endolymphatic hydrops (EH) by MRI is used additionally for the diagnosis of Morbus Menière. However an EH can also be found in other inner ear diseases with different otologic symptoms. Changes of the hydrops over time are rarely examined so far since in most cases imaging is only performed once.
Method: MRI of the temporal bone to detect EH was performed in 200 patients with otologic symptoms. We correlated their clinical diagnosis, the time since onset of symptoms and the number of experienced sudden hearing losses with the grade of the EH. We used four degrees to describe the cochlear hydrops: 1 = apical hydrops visible, 2 = apical and middle turn, 3 = 2 and part of the basal turn involved, 4 = complete cochlea involved.
Results: 38 patients were excluded for tumor, insufficient image quality (movement) and enhancement, leaving 162 patients (324 ears) to be finally evaluated. The extent of the hydrops was increasing with the time since onset of symptoms ($p <= 0.05$) as well as with the number of the events with sudden hearing loss ($p <= 0.05$). The correlation of hydrops extent and the diagnosis of Morbus Menière see Fig. 1.
Conclusion: With time since onset of symptoms the extent of the EH increases. A positive correlation of hydrops extent and the certainty of the clinical diagnosis is given.

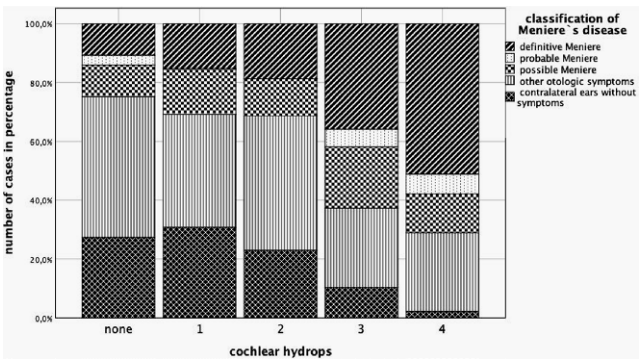

Fig. 1

E-Poster

[1] High-Resolution Gadolinium-Enhanced MR Cisternography Using Compressed-Sensing (CS) T1 SPACE Technique for Detection of Intracranial CSF Leaks

Ikram Eda Duman[1], Theo Demerath[1], Andrea Stadler[1], Samer Elsheikh[1], Esther Raithel[2], Christoph Forman[2], Tanja Hildenbrand[3], Mukesch Shah[4], Jürgen Grauvogel[4]; Christian Scheiwe[4], Horst Urbach[1], Stephan Meckel[1]

[1]Department of Neuroradiology, Medical Center–University of Freiburg, Germany
[2]Siemens Healthcare GmbH, Erlangen, Germany
[3]Department of Otorhinolaryngology, Medical Center–University of Freiburg, Germany
[4]Department of Neurosurgery, Medical Center, Germany

Background & Purpose: In patients with cranial cerebrospinal fluid leaks, precise identification of leakage site is crucial for surgical approach. High-resolution CT cisternography (CTC) is limited in the ability to demonstrate the site of a CSF leak, particularly in patients with multiple or small osseous defects or inactive leaks during imaging. We aimed to test the feasibility of a novel high-resolution gadolinium-enhanced compressed-sensing SPACE technique for MR cisternography (MRC) and to compare findings to CTC and intraoperative results.
Methods: Between November 2019 and March 2020, seven patients with CSF rhinorrhea were studied with CTC and MRC. For MRC, a highly accelerated CS T1 SPACE sequence was applied on a 3 T whole-body MR scanner using a 64-channel head/neck coil. Syngo. via software is used to overlay 3D CS T1 SPACE and CTC images to delineate areas of leaks. Findings of CS SPACE MRC were compared to standard CTC images and intra-operative results.
Results: All CSF leaks were precisely depicted on CS T1 SPACE images (Fig. 1). In five CTC studies, leaks were missed ($n=1$), falsely located ($n=1$), or only suspected ($n=3$). All CSF leaks detected on MRC correlated with findings at surgical repair.
Conclusion: High-resolution gadolinium-enhanced CS T1 SPACE MRC is a promising method for detection of CSF leaks in patients with CSF rhinorrhea. In our pilot experience, this technique appears superior to standard CTC.

[2] Intraarterial Clot Localization in Patients with Acute Ischemic Stroke Affects the Venous Microperfusion Profile'

TD Faizy[1,3], R Kabiri[1,3], M Leipzig[1], S Christensen[2], G Broocks[3], F Flottmann[3], H Leischner[3], M Lansberg2, G Albers[2], J Fiehler[3], M Wintermark[1], JJ Heit[1]

[1]Department of Radiology, Stanford University School of Medicine, CA
[2]Department of Neurology and Neurological Sciences, Stanford University School of Medicine, CA
[3]Department of Neuroradiology, University Medical Center Hamburg-Eppendorf, Germany

Purpose: The quality of cerebral microperfusion (CM) is strongly related to vessel occlusion location and the robustness of arterial intracranial collaterals (IC) in patients with acute ischemic stroke due to large vessel occlusion (AIS-LVO). Robust CM allows for transit of blood through the ischemic brain tissue into the veins. The venous microcirculation profile (VMP) may more accurately reflect tissue perfusion compared to arterial IC, but it is unclear to what extent the venous CM profile is affected by arterial clot localization during AIS-LVO. We determined, if the arterial vessel occlusion localizations predict VMP profile in AIS-LVO patients.
Materials and Methods: We performed a multicenter retrospective cohort study of consecutive patients who underwent thrombectomy for AIS-LVO treatment. Patient details were obtained from prospectively maintained stroke databases and the electronic medical record. Baseline CT angiography was used to localize vessel occlusion, which was dichotomized into proximal (internal carotid artery and proximal M1) and distal (distal M1 and M2) occlusions. The primary outcome measure was VMP, which was determined on baseline CTA by the cortical vein opacification score (COVES). COVES venous opacification was scored for the vein of Labbé, sphenoparietal sinus, and superficial middle cerebral vein were scored as: 0, not visible; 1, moderate opacification; and 2, full opacification.
Results: 374 patients met inclusion criteria. Median age was 76 (IQR: 65–82) and 49 % were female. 196 patients (52 %) had a proximal occlusion and 178 patients (48 %) had a distal occlusion. Median COVES was 1 (range 0–5) for proximal occlusion and 3 (range 0–6) for distal occlusion patients. Mann-Whitney-U tests indicated a significant difference between proximal and distal occlusions ($p<0.001$). Ordinal logistic regression showed that patients with more distal vs proximal occlusions had increased odds of having higher COVES (OR = 12.62,

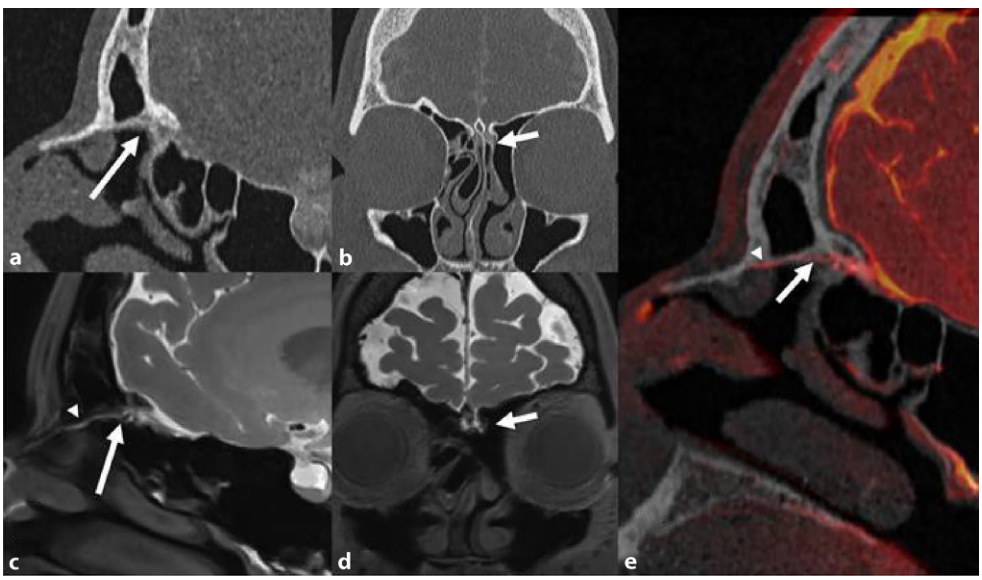

Fig. 1 A 55-year-old female who was re-admitted for recurrent spontaneous left-sided CSF rhinorrhea and persistent slight headaches after previous endoscopic sinus surgery. CT cisternography is unremarkable (**a, b** *arrows*). CS SPACE MR cisternography demonstrates a subtle CSF leak originating from the anterior rim of the left cribriform plate near foramen caecum (**c, d** *arrows*) with a thin CSF collection extending to the anterior nasal cavity (*arrowheads* in **c, e**)

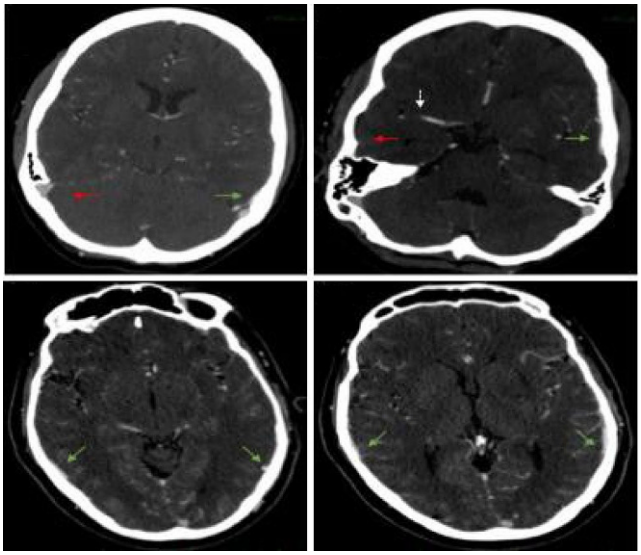

Fig. 1 displays examples of cortical vein opacification scores (COVES) in 2 different patients suffering from proximal (top row, patient 1, dotted white arrow) and distal (bottom row, patient 2) large vessel occlusion. Red arrows indicate poor venous opacification, whereas green arrows represent higher COVES represented by strong vessel opacification.). No visible opacification was detected in the vein of Labe on the right side, whereas strong opacification over the full length of the vein was detected on the left side (COVES 0 right, COVES 2 left). In patient 2, strong opacification of the veins of Labe was found on both hemispheres (COVES 2 on both sides)

[95 % CI 8.02–20.22]; $p<0.001$), independent of age or presentation NIHSS.
Conclusion: The distinct arterial clot localization in AIS-LVO patients affects the cortical venous microperfusion profile. Venous microperfusion was found to be impaired in patients with proximal versus distal vessel occlusions.

[4] Favorable Venous Microperfusion Profile Correlates with Pial Arterial Collateral Status and Clinical Outcome in Acute Stroke Patients with Large Vessel Occlusion

TD Faizy[1,3], R Kabiri[1,3], M Leipzig[1], S Christensen[2], G Broocks[3], F Flottmann[3], M Lansberg[2], G Albers[2], J Fiehler[3], M Wintermark[1], JJ Heit[1]

[1]Department of Radiology, Stanford University School of Medicine, CA
[2]Department of Neurology and Neurological Sciences, Stanford University School of Medicine, CA
[3]Department of Neuroradiology, University Medical Center Hamburg-Eppendorf, Germany

Purpose: Robust pial arterial collaterals (PAC) preserve blood flow to critically hypoperfused brain tissue in patients with acute ischemic stroke due to large vessel occlusion (AIS-LVO). CT angiography (CTA) based methods of pial collateral assessment do not provide tissue level perfusion information, and prior studies have shown that PAC assessment on CT perfusion imaging strongly predicts outcome in AIS-LVO patients treated by thrombectomy. Patients with favorable pial collaterals and brain tissue perfusion also likely have robust cortical venous drainage relative to patients with more impaired cerebral perfusion. We determined the venous microperfusion profile (VMP) in AIS-LVO patients. We hypothesized that robust PAC on CT perfusion predict robust cortical venous contrast opacification on pre-treatment CTA and that a favorable VMP is associated with good clinical outcomes in AIS-LVO patients.
Materials and Methods: We performed a multicenter retrospective cohort study of consecutive AIS-LVO patients who underwent thrombectomy. Included patients had interpretable pre-thrombectomy CT angiography (CTA) and CT perfusion (CTP) studies and clinical outcome data. Patient details were obtained from prospectively maintained stroke databases and the electronic medical record. Pre-thrombectomy CTA and CTP studies were reviewed and scored for tissue-level collaterals using the Hypoperfusion Intensity Ratio (HIR). HIR was defined as the volume ratio of brain tissue with [Tmax>10 sec/Tmax>6 sec] such that a lower HIR correlates with favorable collaterals. HIR was automatically calculated by RAPID (iSchemaView). VMP was determined by opacification of the vein of Labbé, sphenoparietal sinus, and superficial middle cerebral vein on CTA as: 0, not visible; 1, moderate opacification; and 2, full. Primary outcome measure was VMP. Secondary outcome measure was ordinal modified Rankin Scale (mRS). Ordinal linear regression models were performed to predict the effect of HIR on VMP, as well as the effect of VMP on mRS.
Results: 186 patients met inclusion criteria. HIR was dichotomized into lower (≤ 0.4, good collaterals) and higher (≥ 0.5, poor collaterals) ratios. Mann-Whitney-U test indicated that subjects with higher HIR (median COVES = 1) had lower VMP than patients with lower HIR (median COVES = 3) ($p<0.001$). In an ordinal logistic regression model, we tested the effects of VMP on mRS at 90 days after discharge while controlling for HIR (non-dichotomized), age, and TICI score. High (favorable) VMP predicted lower (favorable) mRS (OR = 0.544, [95 % CI 0.4–0.7]; $p=0.032$), which indicates that patients with robust VMP had better neurological outcomes 90 days after discharge.
Conclusion: A robust cerebral venous microperfusion profile reflects greater tissue microperfusion, good arterial collateralization status and is associated with improved clinical outcome in patients with AIS.

[6] Measuring the Head Circumference on MRI

Rau A[1], Demerath T[1], Kremers N[1], Eckenweiler M[2], von der Warth R[3], Urbach H[1]

[1]Dept. of Neuroradiology, University Medical Center Freiburg
[2]Dept. of Neuropediatrics and Muscle Disorders, Medical Center Freiburg
[3]Institute of Medical Biometry and Statistics, University Medical Center Freiburg

Background & Purpose: In order to estimate the brain and head size the head circumference is typically used as a surrogate parameter. As MRI images can be freely zoomed, visual analysis often relies on "impressions" such as the craniofacial ratio or a simplified gyral pattern. Aim of this study was to validate a MRI-based method to measure the head circumference.
Methods: Head circumferences of 85 children (41 micro-, 22 macrocephalies, 22 normal controls) were retrospectively calculated using a 3D-T1w (MPRAGE) data set. Three readers independently placed an ovoid ROI in an axial plane starting from the supraorbital bulge and covering the largest supra-auricular head circumference. Clinical measurements of the head circumference served as ground truth.
Results: Mean deviation from clinical measurements was 6 mm or 1.3 %, respectively. Inter-observer deviations were between 5 and 9 mm. 41 of 41 microcephalies and 19 of 22 macrocephalies were reliably detected. Two patients having head circumferences at the 93rd and 95th percentiles were falsely classified as macrocephalies.
Conclusion: The head circumference can be reliably determined with a simple measurement on 3D sequences using multiplanar reformations. This approach may help to diagnose a micro- or macroecephaly, especially when the head circumference is not reported by the referring clinician.

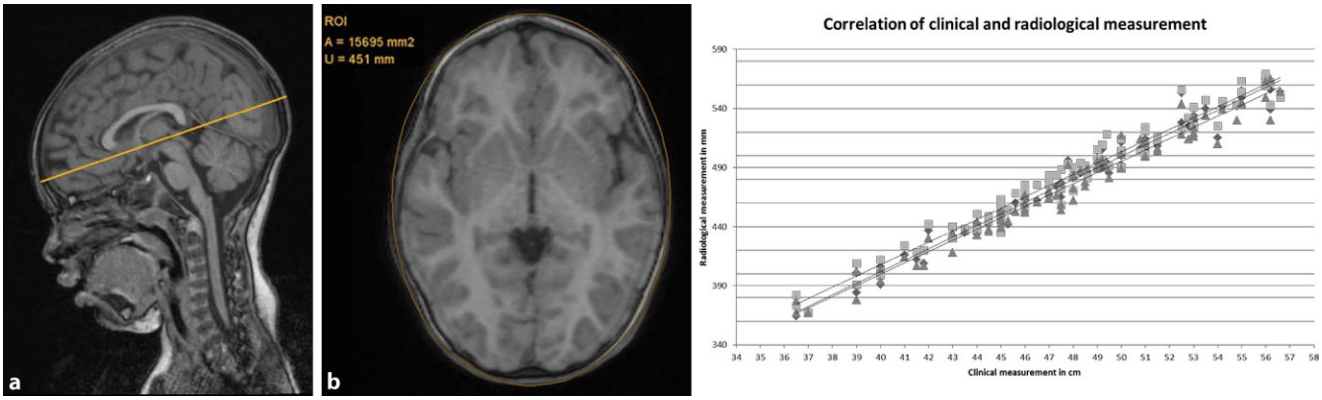

Fig. 1 2 years old girl with microcephaly (clinical head circumference 45 cm/<1st percentile) **a** Mid sagittal MPRAGE slice with a nearly normal craniofacial ratio. **b** Ovoid ROI placement on an axial slice which covers the supraorbital bulge and the largest supra-auricular head circumference (**a** *yellow line*). Radiological head circumference is 45.1 cm

[11] De-Novo Dural Arterio-Venous Fistula Formation Secondary to Cerebral Venous Thrombosis–Longitudinal MRI Assessment Using 4D-Combo-MR-Venography

Schuchardt F[1], Demerath T[2], Elsheikh S[2], Wehrum T[1], Harloff A[1], Urbach H[2], Meckel S[2]

[1]Clinic of Neurology and Neurophysiology, Medical Center–University of Freiburg, Faculty of Medicine, University of Freiburg, Germany;
[2]Department of Neuroradiology, Medical Center–University of Freiburg, Faculty of Medicine, University of Freiburg, Germany

Background and Purpose: Dural arteriovenous fistulae (DAVF) can develop secondary to cerebral venous thrombosis (CVT). The incidence of DAVF has not yet been investigated prospectively.
Methods: Between 07/2012 and 01/2018, combined static and dynamic 4D MR venography (4D-combo-MRV) was performed in 24 consecutive patients with CVT at the time of diagnosis and after 6 months.

3 T MRI with TOF and contrast-enhanced MPRAGE were performed at baseline to evaluate the extent of thrombosis and vessel segments affected. Baseline and follow-up 4D combo MRV data were assessed for signs of a DAVF. Inter-rater reliability of DAVF detection and the extent of recanalization were analyzed with kappa statistics.
Results: DAVF were detected in 4/24 CVT patients (16.7 %). 2/24 (8.3 %) had coincidental DAVF with CVT on admission. At follow-up, de novo formation of DAVF following CVT were seen in 2/24 patients (8.3 %). Both de-novo DAVF were low grade and benign fistulae (Cognard type 1, 2a), which had developed at previously thrombosed segments. Endovascular treatment was required in two DAVF detected at baseline for high degree lesions (Cognard 2a,b) and in one de-novo DAVF (Cognard 1) due to debilitating headache and tinnitus. Thrombus load, vessel recanalization, and frequency of cerebral lesions (hemorrhage, ischemia) were not associated with the occurrence of DAVF.
Conclusions: De-novo DAVF formation occurred more frequently than previously described. Although de-novo DAVF were benign, 75 % of all detected DAVF required endovascular treatment. Therefore, screening for DAVF seems worthwhile in patients with CVT and can be performed using dynamic MRV, such as 4D-combo-MRV.

[13] Application of an Ultra-Short MRI Protocol for Cerebral Staging of Melanoma Patients

Sönke Peters, Friederike Austein, Johannes Hensler, Fritz Wodarg, Olav Jansen

Department of Radiology and Neuroradiology, University Medical Center Schleswig-Holstein (UKSH), Kiel University, Kiel, Germany

Background & Purpose: Due to its high sensitivity MRI is an often used tool for cerebral staging in tumor patients. Contrary to this the relatively long examination times and the limited availability of MRI slots might lead to delayed examinations. Aim of this study was to compare an ultra-short MRI protocol to the routinely used standard protocol.
Methods: Two radiologists retrospectively evaluated two sequences of a cerebral MRI (Flair images and contrast enhanced T1 MPR images) of 147 patients with malignant melanoma. The results were compared to the report of the full MRI examination and a statistical testing for non-inferiority was performed.
Results: 12.93 % of the patients had cerebral metastases. Overall 79 Metastases were detected, 65 were located supratentorial and 14 were located infratentorial. Concerning the detection of cerebral metastases, the ultra-short MRI examination was not inferior to the full MRI protocol in general ($p = 0.001$) and separated by location for supratentorial ($p < 0.001$) and infratentorial ($p = 0.014$) metastases.
Conclusion: No general recommendations for a MRI screening protocol of neurologic asymptomatic patients with cancer for cerebral metastases exist. Our study shows that an ultra-short MRI protocol for staging purpose is not inferior in detecting cerebral melanoma metastases to the routine MRI protocol. Even though a cerebral staging in neurologic asymptomatic patients is not necessary in early tumor stages, a rising demand for cerebral imaging can be expected due to a rising incidence of neoplastic diseases (1). Shorter and faster MRI examinations could be the key for a more efficient use of the often restricted MRI capacities.

References

1. Global Burden of Disease Cancer Collaboration, Fitzmaurice C et al. Global, Regional, and National Cancer Incidence, Mortality, Years of Life Lost, Years Lived With Disability, and Disability-Adjusted Life-years for 32 Cancer Groups, 1990 to 2015: A Systematic Analysis for the Global Burden of Disease Study. JAMA Oncol. 2017 Apr 1;3(4):524–48.

[14] Determining Lactate Gradients in Glioblastomas with MRI Multi Voxel Spectroscopy

Sönke Peters[1], Carolin Kubelt[2], Monika Huhndorf[1], Lukas Huber[3], Janka Held-Feindt[2], Michael Synowitz[2], Olav Jansen[1], Jan-Bernd Hövener[3]

[1]Department of Radiology and Neuroradiology, University Medical Center Schleswig-Holstein (UKSH), Kiel University, Kiel, Germany;
[2]Department of Neurosurgery, University Medical Center Schleswig-Holstein (UKSH), Kiel University, Kiel, Germany;
[3]Section for Biomedical Imaging, Molecular Imaging North Competence Center (MOIN CC), Department of Radiology and Neuroradiology, University Medical Center Schleswig-Holstein (UKSH), Kiel University, Kiel, Germany

Background & Purpose: Glioblastoma (GBM) is characterized by an infiltrative growth. Aim of this study was to verify this diffuse infiltration with multi voxel spectroscopy (MVS) MRI by evaluating lactate.
Methods: Patients with suspected GBM underwent a MVS at 3 T (CSI PRESS; TE = 288 ms; TR = 1500 ms; voxel size 10 × 10 × 10 mm) before surgery. The lactate concentrations of different regions were determined: "tumor" = contrast enhancing part; "edema" = edema with-out contrast enhancement and "normal appearing white matter" (NAWM) = next to the edema.
Results: 8 MRI of histological proven GBM with IDH-wildtype were evaluated. In all cases lactate was detected in the defined regions, even though the measured lactate concentrations were on different levels for each patient. Taken the "tumor" area as 100 %, relative concentrations of 47.78 % (SD 9.52 %) in the "edema" and of 6.11 % (SD 1.94 %) in the "NAWM" were comparable.
Conclusion: Lactate accumulates in cancer and can reflect the tumor infiltration. To get a better lactate signal, a TE of 288 ms was chosen (1).

Interestingly, different levels of lactate concentrations in between patients were detectable, whereas the relative changes of the lactate concentrations among the defined regions are comparable.

The infiltrative growth of GBM is reflected by a lactate gradient as monitored by MVS. Further studies must clarify in more detail whether these finding have a prognostic impact and can be used for therapy monitoring.

References

1. Lange et al. Pitfalls in lactate measurements at 3T. AJNR 2006 Apr;27(4):895–901.

[16] Spatial Metabolic Correlations as Indication of possible Metabolic Connectivity Networks–A Short Echo-Time Whole-Brain MR Spectroscopic Imaging Study

Ahlswede M, Maghsudi H, Fu T, Nösel P, Schütze M, Dadak M, Lanfermann H, Ding XQ

Institut für Diagnostische und Interventionelle Neuroradiologie, Medizinische Hochschule

Background & Purpose: While it is well known that the brain functions as a network, little is known concerning metabolic connectivity within the human brain. We aimed to uncover possible brain metabolic connectivity by determination of correlations between regional metabolite concentrations.
Methods: Based on the data acquired with short echo-time whole-brain MR spectroscopic imaging from 55 healthy subjects at 3 T, N-acetylaspartate (NAA), total choline (tCho), total creatine (tCr), glutamine and glutamate (Glx), and myo-Inositol (mI) concentrations were measured in 12 regions of interest (ROIs). Pearson's correlation test was performed to assess spatial correlations between regional metabolite concentrations.
Results: Significant spatial correlations were found in several brain regions for metabolites NAA, tCho, Glx and mI. The most frequent metabolic correlations were occurred in the ROI of posterior limb of the internal capsule, i. e. to putamen for NAA and Glx, to centrum semioval for tCho and mI, to subcortical motor areal and parietal white matter for tCho, and to frontal white matter for mI; and the most spatial metabolic correlations were found for metabolite mI.
Conclusion: Our preliminary results indicated possible metabolic connectivity networks in human brain. Future studies are needed to validate present results.

[17] Brain Metabolic Alterations in Patients Shortly After Liver Transplantation

Patrick Nösel[1*], Henning Pflugrad[2,3*], Wolfgang Knitsch[4], Heinrich Lanfermann[1], Elmar Jäckel[3,5], Hannelore Barg-Hock[4], Jürgen Klempnauer[3,4], Karin Weissenborn[2,3#], Xiao-Qi Ding[1#]

[1]Institute of Diagnostic and Interventional Neuroradiology, Hannover Medical School, Hannover;
[2]Department of Neurology
[3]Integrated Research and Treatment Centre Transplantation
[4]Clinic for Visceral and Transplant Surgery
[5]Clinic for Gastroenterology, Hepatology and Endocrinology
*/# equal first and last authorship

Background & Purpose: In the first few weeks after a liver transplantation (LTx) some patients present neurological abnormalities like impaired consciousness, confusion, hallucination and/or seizures, while their standard brain MR images did not show abnormal findings. Therefore a metabolic-toxically cause is currently assumed for the post-transplant encephalopathy (PTE), but the underlying pathomechanism is not yet clarified.
Methods: 36 patients, 28 of them without PTE (Group P1) and 8 with PTE (Group P2) underwent shortly after LTx (within two weeks) phosphor 31 magnetic resonance spectroscopy examinations. The concentrations of metabolites Adenosintriphosphat (ATP), Phosphocreatin (PCr), Nicotinamidadenindinukleotid (NAD), Phosphodiester (PDE), Phosphomonoester (PME) and inorganic Phosphat (Pi) were determined. The results of the patient groups (P1 & P2) have been compared to those of a healthy control group (HC).
Results: Our preliminary results showed that in comparison to the HC, both patients groups showed lowered ATP, increased PCr and PDE concentrations, but more distinct in patients with PTE, who revealed additionally decreased PME.
Conclusion: Our first results showed alterations of brain metabolism in LTx patients. The special metabolic changes in P2 group indicated a possible participation of the cerebral metabolism in genesis of PTE.

[18] Neuromorphological Findings in Patients with 22q11.2 Deletion Syndrome

Neuhaus E[1,2], Hattingen E[1], Breuer S[1], Steidl E[1], Polomac N[1], Rosenow F[2], Ecker C[3,4], Bearden CE[5], Kushan L[5], Lin A[5], Vajddi A[5], Jurcoane A[1]

[1]Institute of Neuroradiology, Goethe University Frankfurt, Frankfurt am Main, Germany
[2]Department of Neurology and Epilepsy Center Frankfurt Rhine-Main, Goethe University Frankfurt, Frankfurt am Main, Germany; LOEWE Center for Personalized Translational Epilepsy Research (CePTER), Goethe University Frankfurt, Frankfurt am Main, Germany
[3]Department of Child and Adolescent Psychiatry, Psychosomatics and Psychotherapy, Goethe University Frankfurt, Frankfurt am Main, Germany
[4]Department of Forensic and Neurodevelopmental Sciences; Institute of Psychiatry, Psychology and Neuroscience; King's College, London

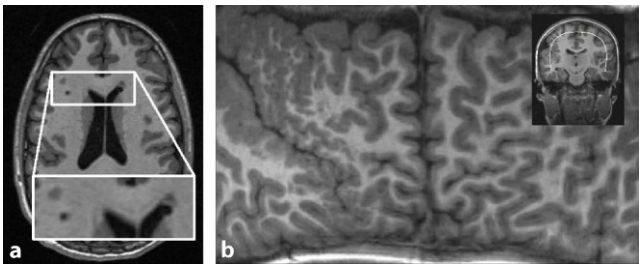

Fig. 1 **a** Heterotopias and cysts (located periventricular and in frontal white matter), **b** Mercator brain map of unilateral right polymicrogyria in the perisylvian area

[5]Department of Psychiatry and Biobehavioral Sciences, Semel Institute for Neuroscience and Human Behavior and Department of Psychology, University of California-Los Angeles, Los Angeles, CA, USA

Background & Purpose: MRI studies and neuropathological findings in patients with 22q11.2 deletion syndrome (22q11.2DS), which is the most common microdeletion syndrome [1], suggest anomalous early brain development [2, 3]. We aimed to evaluate morphological abnormalities of the brain in patients with 22q11.2DS and to correlate these with the most common neuropsychiatric impairments.
Methods: Morphological abnormalities were assessed based on 3D T1-weighted images in 75 patients with 22q11.2DS and in 53 demographically matched controls. Three raters, blinded for disease status and for expected MR findings, identified all individuals with gray matter heterotopias and other morphological brain abnormalities. Moreover, we examined the association between the most frequent morphological findings, general cognitive performance, and co-morbid neuropsychiatric conditions.
Results: Nodular heterotopia (periventricular or in the white matter) were the most frequent findings in patients ($n=33$; controls $n=4$, $p<0.001$), followed by cavum septi pellucidi et vergae ($n=20$; controls $n=0$, $p<0.001$), dysmorphic small neurocranium ($n=17$; controls $n=1$, $p=0.002$), and periventricular cysts ($n=11$; controls $n=0$, $p<0.005$). Three patients had unilateral polymicrogyria (Fig. 1). There was no difference in psychiatric or cognitive behavior between patients with and without these morphological brain abnormalities.
Conclusion: MR morphological manifestations in patients with 22q11.2DS are frequent and not related to psychiatric or cognitive manifestations. MR morphological signs of impaired brain development seem to be indicative for the pathogenesis of 22q11.2DS, but they are not a surrogate for its clinical severity.

References

1. McDonald-McGinn, D.M., et al., *22q11.2 deletion syndrome.* Nat Rev Dis Primers, 2015.
2. Schmitt, J.E., et al., *Incidental radiologic findings in the 22q11.2 deletion syndrome.* AJNR Am J Neuroradiol, 2014.
3. Rezazadeh, A., et al., *Periventricular nodular heterotopia in 22q11.2 deletion and frontal lobe migration.* Ann Clin Transl Neurol, 2018.

[19] Hemodynamic Evaluation of Patients with Moyamoya: Comparison of Resting-State-fMRI to Breath-Hold-fMRI

Zerweck L[1], Hauser TK[1], Roder C[2], Ernemann U[1], Klose U[1]

[1]Department of Neuroradiology; University Hospital Tuebingen
[2]Department of Neurosurgery; University Hospital Tuebingen

Background & Purpose: Patients with Moyamoya Disease (MMD) require the estimation of remaining cerebrovascular reactivity (CVR), for example by breath-hold(bh)-triggered-fMRI [1]. Recent findings suggest the use of resting-state (rs)-fMRI [2]. The aim of this study was to compare rs-fMRI to bh-fMRI.
Methods: rs- and bh-fMRI data sets of 7 MMD patients were realigned, normalized, segmented into 6 standardized ROIs [3] and spatially smoothed. The bh-images were additionally slice-time corrected. The rs-data was temporally band-pass filtered (0.02–0.04 Hz). bh-CVR-maps (Fig. 1b) were calculated by voxel-wise integrating the signal time-course and rs-CVR-maps (Fig. 1a) were calculated by linear regression analysis in which the cerebellar time-course was the regressor. We compared the mean CVR of the 6 ROIs (Fig. 2a) of all patients.
Results: The CVR-maps of both modalities showed high correlation (correlation coefficient = 0.80, $p<0.001$, Fig. 2b).
Conclusion: rs-fMRI seems to be a promising method for hemodynamic evaluation. It requires minimum patient compliance and no complex equipment.

References

1. Hauser et al. Hypercapnic BOLD-MRI compared to H2 OPET/CT for the hemodynamic evaluation of patients with Moyamoya Disease. NeuroimageClin22:101713.
2. Liu et al. Cerebrovascular reactivity mapping without gas challenges. Neuroimage146:320–326.
3. Tatu et al. Arterial territories of the human brain:cerebral hemispheres. Neurology50:1699–1708.

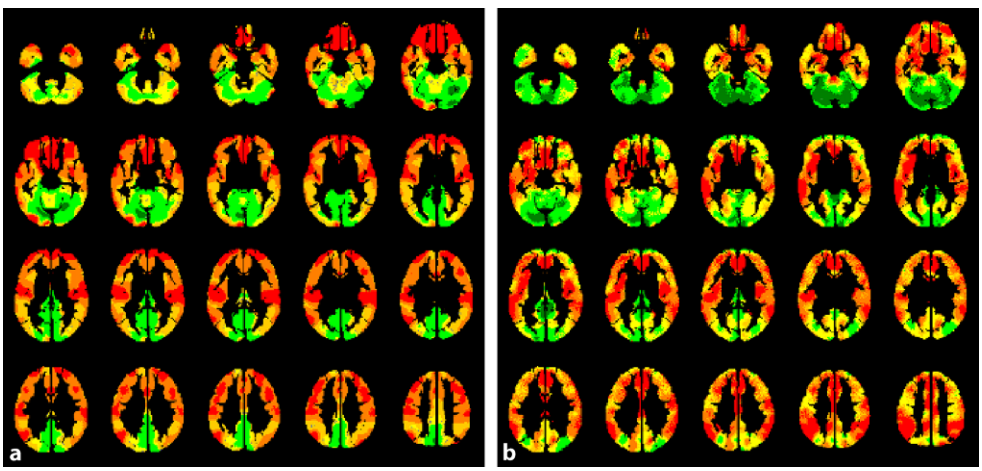

Fig. 1 CVR-maps of an exemplary patient gained by bh- (**a**) and rs-fMRI (**b**). Low/high CVR is represented by warm/cold colors

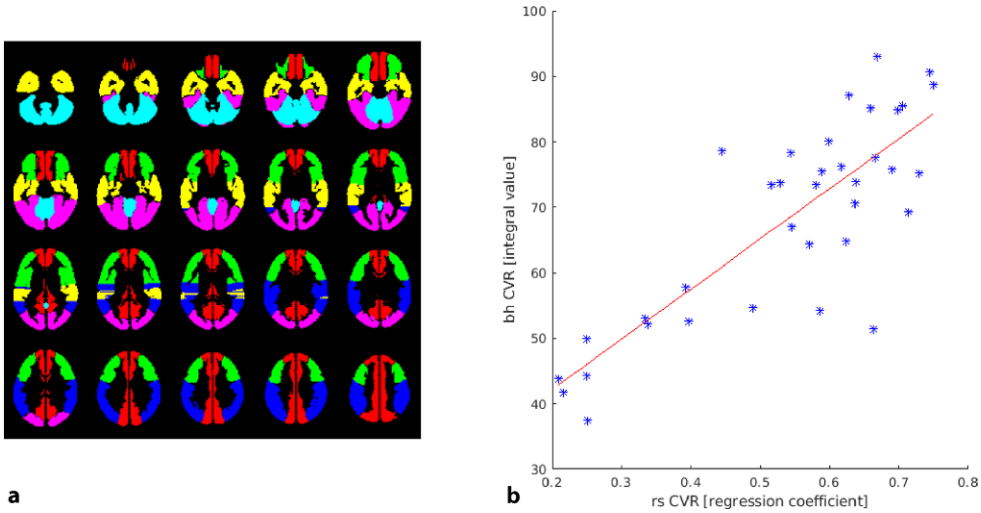

Fig. 2 Evaluated ROIs (**a**) and correlation between rs- and bh-fMRI (**b**)

[21] Is Pre-Contrast T1-Weighted Imaging of the Spinal Cord Necessary in Patients with Multiple Sclerosis?

Isabelle Riederer[1], Mark Mühlau[2,3], Claus Zimmer[1], Magaly Gutbrod-Fernandez[1], Nico Sollmann[1,2]*, Jan S Kirschke[1]*

(*These authors contributed equally)
[1]Department of Neuroradiology, Klinikum rechts der Isar, School of Medicine, Technical University of Munich, Munich, Germany
[2]TUM-NIC, TUM Neuroimaging Center, Klinikum rechts der Isar, School of Medicine, Technical University of Munich, Munich, Germany
[3]Department of Neurology, Klinikum rechts der Isar, School of Medicine, Technical University of Munich, Munich, Germany

Background & Purpose: Multiple Sclerosis (MS) is an inflammatory disease of the CNS including the spinal cord. Spinal MRI plays an important role for diagnosis and prognosis but can be time-consuming. We hypothesize that pre-contrast T1-w imaging does not add diagnostic value and thus could be excluded to reduce scan time.
Methods: 3 T MRI scans including sagittal and axial T2-w images and sagittal pre- and post-contrast T1-w images of 265 consecutive patients with (suspected) MS were analyzed retrospectively. Two neuroradiologists independently assessed the images in two separate reading sessions: first excluding and second including pre-contrast T1-w images. Number of contrast-enhancing (ce) lesions as well as diagnostic confidence, overall image quality and artifacts were rated on Likert scales. The results were compared using Wilcoxon signed-rank test and weighted Cohen's kappa.
Results: All 56 ce lesions found in 43 patients in the first reading could be identified as well in the second image analysis when including pre-contrast T1-w images. Additionally, there were no false positives when excluding pre-contrast images and no significant differences in diagnostic confidence between both image analyses for both readers (reader 1: $p=0.058$; reader 2: $p=0.317$). Inter-rater concordance was both moderate regarding artifacts (κ: 0.418) and overall image quality (κ: 0.504).
Conclusions: Presence of pre-contrast T1-w images did not significantly increase detection rate or diagnostic confidence of ce lesions in the spinal cord in patients with MS and might, therefore, be skipped in routine spinal MRI protocol in MS patients to reduce scan duration and increase patient's compliance.

[24] Correlation of Qualitative And Quantitative MRI Parameters for Assessment of Fatty Infiltration in Patients with Neuromuscular Diseases

S. Schlaeger[1], N. Sollmann[1,2], A. Zoffl[1], D. Weidlich[3], E. Klupp[1,3], I. Riederer[1], M. Dieckmeyer[1], J. Syvaeri[3], T. Greve[1], E. Burian[1], F. Montagnese[4], M. Deschauer[5], B. Schoser[4], S. Bublitz[5], C. Zimmer[1,2], D.C. Karampinos[3], T. Baum[1], J.S. Kirschke[1,2]

[1]Department of Diagnostic and Interventional Neuroradiology, Klinikum rechts der Isar, Technische Universität München, Munich, Germany
[2]TUM-Neuroimaging Center, Klinikum rechts der Isar, Technische Universität München, Munich, Germany
[3]Department of Diagnostic and Interventional Radiology, Klinikum rechts der Isar, Technische Universität München, Munich, Germany
[4]Friedrich-Baur-Institut, Department of Neurology, Ludwig-Maximilians-Universität, Munich, Germany
[5]Department of Neurology, Klinikum rechts der Isar, Technische Universität München, Munich, Germany

Background & Purpose: The musculature of patients suffering from neuromuscular diseases (NMD) is mainly affected by atrophy/hypertrophy, fatty infiltration, and/or edematous changes [1]. Therefore, MRI is an important tool for diagnosis and monitoring. Concerning fatty infiltration, standard T1-weighted or T2-weighted DIXON TSE sequences enable a qualitative assessment of muscle involvement [2]. To achieve higher comparability semi-quantitative grading scales, such as the 4-point Mercuri scale [3], can be applied. However, the evaluation remains dependent on the reader's judgment. Therefore, effort is being invested to develop quantitative MRI techniques, such as proton density fat fraction (PDFF) mapping. The present work aims to assess the diagnostic value of PDFF mapping in correlation to Mercuri grading in patients with DM2, LGMD2A, and Pompe disease.
Methods: T2-weighted DIXON TSE and PDFF mapping were performed in 13 patients (DM2: $n=5$; LGMD2A: $n=5$; Pompe disease: $n=3$). Nine different thigh muscles were rated in all patients according to the Mercuri grading and segmented to extract PDFF values.
Results: Mean PDFF values ranged from 7 to 37 % in Pompe and DM2 patients and up to 79 % in LGMD2A patients (Fig. 1). In all three groups a high correlation of the Mercuri grading and PDFF values was observed (Table 1).
Conclusion: In the investigated patient groups PDFF mapping offers the same diagnostic value as the clinically established Mercuri grading. With its greater dynamic range (enabling the assessment of more subtle

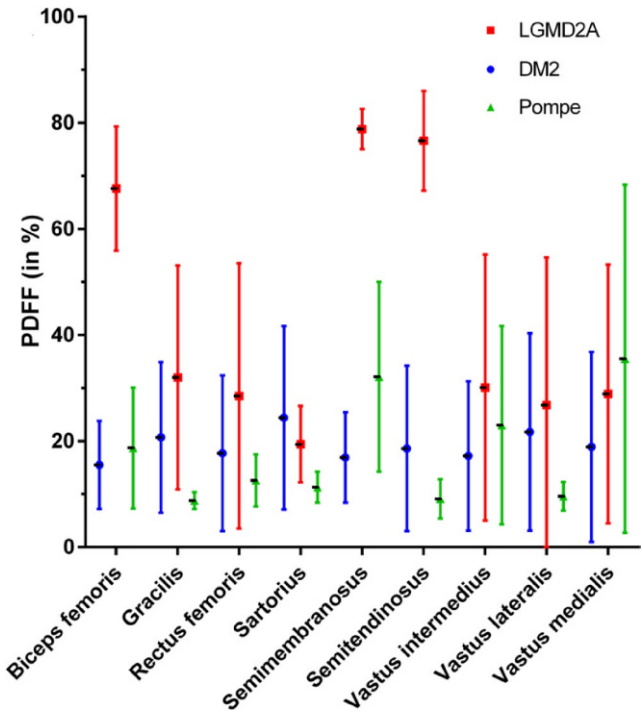

Fig. 1 Extracted PDFF values (%) versus thigh muscles (Spearman correlation coefficient r und p-value)

	PDFF – Mercuri	
	r	p-value
Biceps femoris	n.s.	
Gracilis	0.81	<0.01
Rectus femoris	0.87	<0.01
Sartorius	0.71	0.01
Semimembranosus	0.94	<0.01
Semitendinosus	0.83	<0.01
Vastus intermedius	0.86	<0.01
Vastus lateralis	n.s.	
Vastus medialis	0.87	<0.01

Fig. 2 PDFF values versus Mercuri grades

changes) and the increased objectivity, PDFF should be considered a potential biomarker and alternative to Mercuri grading in the assessment of fatty infiltration of muscle tissue.

References

1. Mercuri, E et al. Muscle imaging in clinical practice: diagnostic value of muscle magnetic resonance imaging in inherited neuromuscular disorders. Current opinion in neurology.
2. Schlaeger, S et al. T2-Weighted Dixon Turbo Spin Echo for Accelerated Simultaneous Grading of Whole-Body Skeletal Muscle Fat Infiltration and Edema in Patients With Neuromuscluar Diseases.J Comput Assist Tomogr.
3. Mercuri, E et al. Musle MRI in inherited neuromuscular disorders: past, present, and future. Journal of Magnetic Resonance Imaging.

[25] KM Index: Prediction of Midline Shift After Middle Cerebral Artery (MCA) Ischemia Using Computed Tomography Perfusion

Müller SJ, Khadhraoui E, Riedel CH

Institute of Neuroradiology, University Medicine Göttingen

Background & Purpose: Timing and necessity of decompressive surgery after potentially malignant infarction in the MCA territory are a frequently debated issue. We introduce the Kinematics of MCA ischemia (KM-) index, which can be calculated based on an initial computed tomography perfusion scan and the chosen therapy (lysis/thrombectomy/conservative), in order to estimate the maximum midline-shift in the subsequent six days.
Methods: We retrospectively analyzed data of 186 patients with MCA territory stroke who had a computed tomography (CT) perfusion scan and CT angiography in the acute setting and who presented in our emergency room between 2015 and 2019. Midline shift was measured on follow-up imaging between days 0 and 6 after stroke. We calculated Pearson's correlation, sensitivity, specificity and receiver operator characteristics between the KM index and the amount of midline shift.
Results: The mean KM index of all patients was 1.01 ± 0.09 (decompressive hemicraniectomy subgroup 1.13 ± 0.13; midline shift subgroup 1.18 ± 0.13). The correlation coefficient between the KM index and substantial midline-shift was 0.61, $p < 0.01$ and between KM index and decompressive hemicraniectomy or death 0.47; $p < 0.05$. KM index>1.02 shows a sensitivity of 92 % (22/24) and a specificity of 78 % (126/162) for detecting midline shifts. The area under curve of the receiver operator characteristics was 91 % for midline shifts and 86 % for the occurrence of decompressive hemicraniectomy or death.
Conclusion: In this retrospective study, our KM index shows a strong correlation with significant midline-shift. Therefore, the KM index may have a potential use in risk stratification regarding the need for decompression surgery.

[26] Novel T1 Mapping of the Whole Brain: Results for Normal Brain Tissue and First Clinical Experience

Müller SJ[1], Khadhraoui E[1], Voit D[2], Riedel CH[1], Frahm J[2]

[1]Institute of Neuroradiology, University of Göttingen
[2]Max Planck Institute for Biophysical Chemistry, Göttingen

Background & Purpose: This study evaluated a novel single-shot T1 mapping method for rapid and accurate multi-slice coverage of the whole brain, described by Wang et al. 2015.
Methods: At a field strength of 3 T T1 mapping of 76 patients and 5 volunteers (two repetitions) was performed at 0.5 mm in-plane resolution, 3 to 4 mm slice thickness and within an acquisition time of 4 s per slice. Mean T1 values were determined in 20 manually segmented regions-of-interest without pathologic findings.
Results: A total of 86 T1 mapping studies were analyzed. Mean age of the cohort was 49 (range 16–91 years). The following T1 relaxation

times (in ms) were observed: grey matter 1261 ± 77 (mean±SD), frontal white matter 771 ± 55, putamen 1079 ± 60, nucleus ruber 850 ± 49, substantia nigra 798 ± 52, pons 845 ± 52, nucleus dentatus 810 ± 53, and cortex cerebelli 1161 ± 98. Intra- and inter-subject reproducibility was excellent, mean coefficient of variations were 2.4 and 3.8 %, respectively. T1 values for pathologies were quantified (in ms): tumor with contrast agent 533 ± 88, tumor edema 1504 ± 196, large microvascular lesions 1203 ± 58, inactive multiple sclerosis lesions 1210 ± 533 and subacute infarction 1389 ± 153.

Conclusion: The novel rapid T1 mapping method emerges as a reliable MRI technique for identifying and quantifying normal brain structures and may thus serve as a basis for assessing pathologies.

References

1. Wang, X. et al.: Single-shot multi-slice T1 mapping at high spatial resolution–Inversion-recovery FLASH with radial undersampling and iterative reconstruction. Open Med Imag J. 9, 1, 1–8 (2015). https://doi.org/10.2174/1874347101509010001.

[27] MRI Characteristics in Treatment for Cerebral Melanoma Metastasis Using Stereotactic Radiosurgery and Concomitant Checkpoint Inhibitors or Targeted Therapeutics

Rauch M[1], Tausch D[1], Blanck O[2], Wolff R[2], Urban H[3], Hattingen E[1]

[1]Institute for Neuroradiology, Johann Wolfgang Goethe University, Frankfurt am Main, Germany
[2]Saphir Radiosurgery Center, Frankfurt am Main, Germany
[3]Institute for Neurooncology, Johann Wolfgang Goethe University, Frankfurt am Main, Germany

Background & Purpose: Combination therapy for melanoma brain metastases (MM) using stereotactic radiosurgery (SRS) and immune checkpoint inhibition (ICI) or targeted therapy (TT) is currently of high interest[1,2]. In this collective, time evolution and incidence of imaging findings indicative of pseudoprogression is sparsely researched. We therefore investigated time-course of MRI characteristics in these patients.

Methods: Data were obtained retrospectively from 27 patients (12 female, 15 male; mean 61 years, total of 169 MMs). Single lesion volumes, total MM burden and edema volumes were analyzed at baseline and follow-up MRIs in 2 months intervals after SRS up to 24 months. The occurrence of intratumoral hemorrhages was recorded.

Results: 17 patients (80 MM) received ICI, 8 (62 MM) TT and 2 (27 MM) ICI+TT concomitantly to SRS. MM-localization was frontal ($n=89$), temporal ($n=23$), parietal ($n=20$), occipital ($n=10$), basal ganglia/thalamus/insula ($n=10$) and cerebellar ($n=10$). A volumetric progression of MM 2–4 months after SRS was observed in combined treatment with ICI ($p=0.028$) and ICI+TT ($p=0.043$), whereas MMs treated with TT showed an early volumetric regression ($p=0.004$). Edema volumes moderately correlated with total MM volumes ($r=0.57$; $p<0.0001$). Volumetric behavior did not differ significantly over time regarding lesions' initial sizes or localizations. No significant differences between groups were observed regarding rates of post-SRS intralesional hemorrhages.

Conclusion: A reversible volumetric increase in terms of pseudoprogression is observed 2–4 months after SRS in patients concomitantly treated with ICI and ICI+TT, rarely after TT. Edema volumes mirror total MM volumes. Medical treatment type does not significantly affect rates of intralesional hemorrhage.

References

1. Gabani P et al. Stereotactic radiosurgery and immunotherapy in melanoma brain metastases: Patterns of care and treatment outcomes. Radiother Oncol J Eur Soc Ther Radiol Oncol. 2018;128(2):266–273

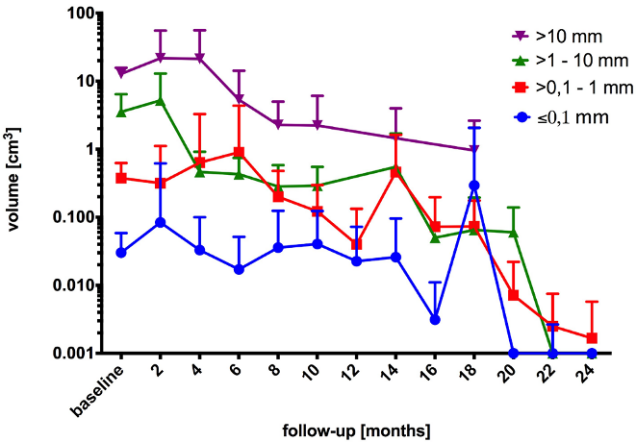

Fig. 1 Time course of MM volumes depending on medical treatment. (*ICI* immune checkpoint inhibitors, *TT* targeted therapy)

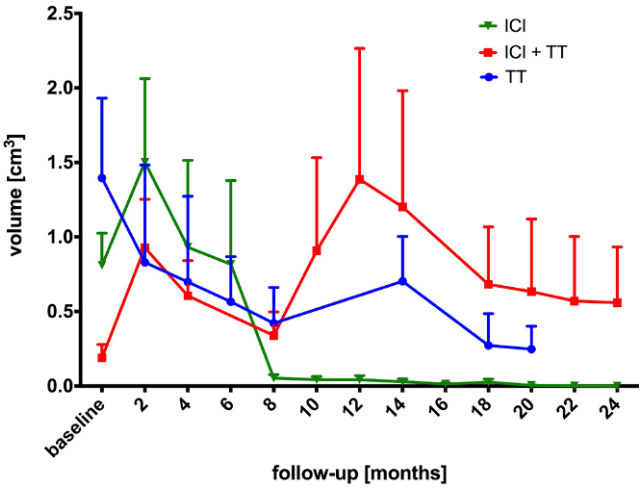

Fig. 2 Volumetric MM time course after SRS regarding initial volumes

2. Kotecha R et al. Melanoma brain metastasis: the impact of stereotactic radiosurgery, BRAF mutational status, and targeted and/or immune-based therapies on treatment outcome. J Neurosurg. 2018;129(1):50–59

[28] Human-Expert-Level Brain Tumor Detection Using Deep Learning with Data Distillation and Augmentation

Lu, D[2], Polomac N[1], Gacheva I[1], Hattingen E[1], Triesch J[2]

[1]Institute of Neuroradiology, Goethe University Frankfurt, Frankfurt am Main, Germany
[2]Frankfurt Institute for Advanced Studies (FIAS) Frankfurt am Main, Germany

Background & Purpose: The application of Deep Learning for medical diagnosis is often hampered by two problems. First, the amount of training data may be scarce, limited by the number of patients diagnosed with the condition. Second, the training data may be corrupted by various types of noise. Here, we study the problem of brain tumor diagnosis with magnetic resonance spectroscopy (MRS) data, where both problems are prominent. To overcome these challenges, we propose a new method for training a deep neural network that distills par-

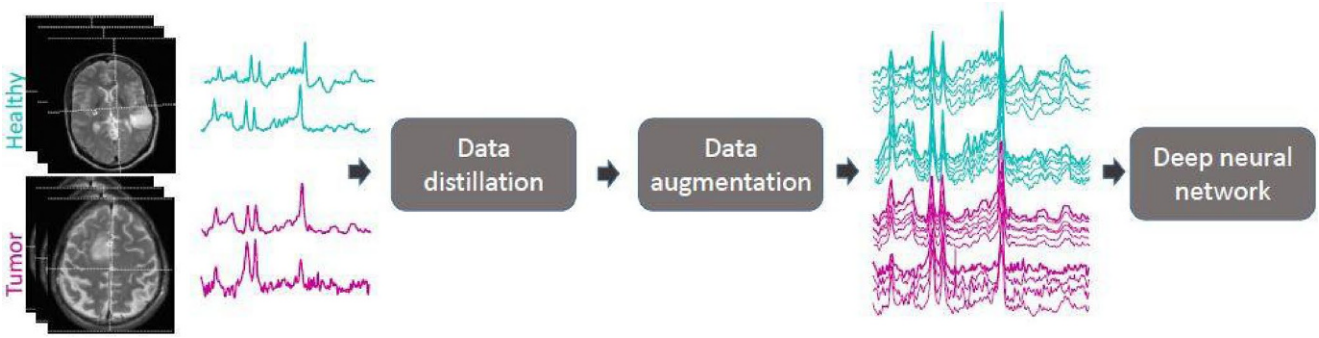

Fig. 1 Overview of the proposed approach

ticularly representative training examples and augments the training data by mixing these samples from one class with those from the same and other classes to create additional training samples.
Methods: 1H-MRS data from 435 patients included 7442 spectra; 3388 of them localized in normal appearing brain tissue and 4054 in brain tumor. These spectra were labeled and used for analysis. Data distillation and data augmentation are used to improve labeling of the spectra and to increase the number of training samples, respectively (Fig. 1). The deep convolutional residual neural network (ResCNN)[1] was used to classify the spectra in the tumor and non-tumor group on the validation set. Human experts also assessed the same validation set.
Results: The proposed algorithm with data augmentation achieved an AUC of 0.77 (solid blue), which encompasses most of the neuroradiologists in the ROC plot (Fig. 2).
Conclusion: We demonstrate that this technique substantially improves performance, allowing our method to reach human-expert-level accuracy with just a few thousand training examples.

References

1. Kaiming He, Xiangyu Zhang, Shaoqing Ren, and Jian Sun. Deep residual learning for image recognition. In Proceedings of the IEEE conference on computer vision and pattern recognition, pages 770–778, 2016.

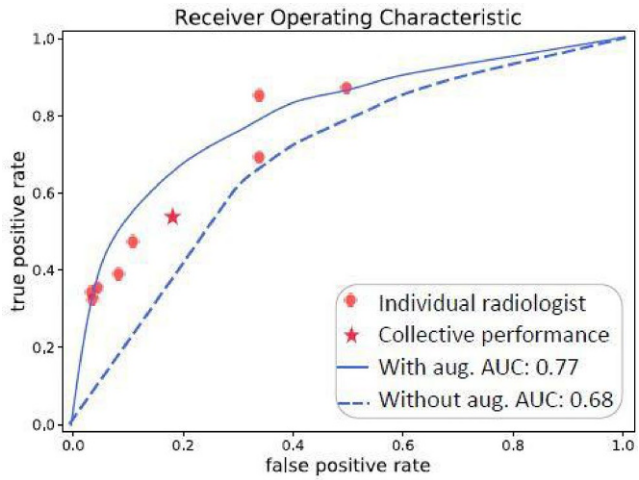

Fig. 2 Comparison of the model and neuroradiologists performance on one randomly selected cross validation set. The individual and collective performance of neuroradiologists are shown as red dots and red star, respectively. The average ROC curve of the plain ResCNN model and our proposed model with augmentation are depicted in dashed and solid blue lines, respectively

[29] Fast Multi-Slice Imaging with CEST-EPI

Jan-Rüdiger Schüre[1], Ulrich Pilatus[1], Ralf Deichmann[2], Elke Hattingen[1], Manoj Shrestha[2]

[1]Department of Neuroradiology
[1]University Hospital Frankfurt, Frankfurt am Main, Germany
[2]Brain Imaging Center (BIC), Goethe University Frankfurt, Frankfurt am Main, Germany

Background & Purpose: APT-CEST imaging allows for assessing tumor infiltration, providing information on protein concentrations and intracellular pH changes[1]. The method acquires a Z-spectrum. This can be time-consuming, especially for a large number of frequency offsets and full tumor coverage. Here, we present a fast multi-slice CEST-EPI sequence, extending the work by Sun et al.[2] via further optimizing the saturation scheme.
Methods: The proposed sequence employs a pre-saturation CEST pulse train, driving the magnetization into a steady-state, followed by a secondary module comprising one CEST pulse and an EPI acquisition, being embedded in a slice and a frequency offset loop. This maintains the steady-state throughout the whole measurement, being faster than the standard scheme which employs pre-saturation for each single frequency offset. Up to 16 slices per volume can be acquired in 8 s (80 mm coverage, in-plane resolution: 3×3 mm^2). The sequence was tested with a maximum increment of 0.5 ppm. Both schemes were compared in-vitro on a phantom with different T1 times and in-vivo.
Result: In-vitro, no significant difference was found via MTRasym(3.5 ppm) (Fig. 1). The comparison in-vivo over 16 slices shows a similar contrast for the white matter as well as for the tumor. Only CSF has a higher signal compared to the proposed sequence (Fig. 2).
Conclusion: The proposed sequence yields a speedup by a factor of two via restriction to a single pre-saturation module. Comparison with the results of the standard scheme revealed no significant differences.

References

1. Kevin J. et al., Tumor pH and Protein Concentration Contribute to the Signal of Amide Proton Transfer, Magnetic Resonance Imaging, 2019
2. Sun et al., Fast multislice pH-weighted chemical exchange saturation transfer (CEST) MRI with Unevenly segmented RF irradiation, Magnetic resonance in medicine, 2011

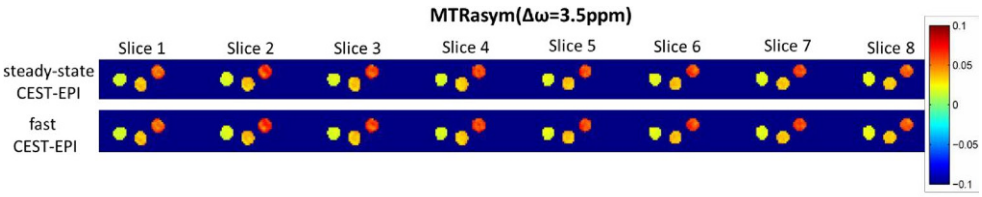

Fig. 1 Sequence validation in-vitro. Eight slices from a phantom with tubes at different T1 relaxation times (f.l.t.r: 450 ms, 850 ms 1300ms) are shown. No significant difference in contrast between both sequences can be detected

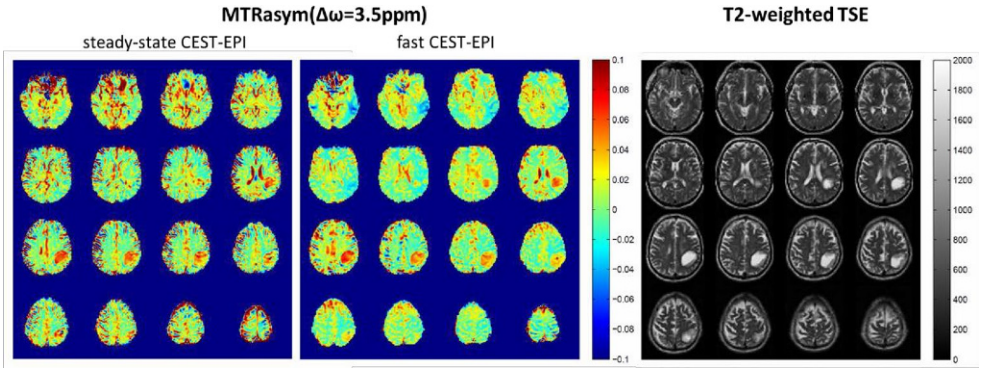

Fig. 2 MTRasym (3.5 ppm) across 16 slices with the standard steady-state and the proposed fast CEST-EPI sequence. Both sequences show a similar contrast regarding the white matter and tumor issue. T2-weighted images are shown on the right panel

[30] Benefits of the Stroke Emergency Mobile (STEMO) for Patients with Large Vessel Oc-clusions of the Anterior Circulation"

Rogge W[1], Mutze S[2,3], Güthoff C[4], Kreissl L[2], Sparenberg P[1], Wendt M[1], Schmehl I[1], Audebert H[5], Goelz L[2,3]

[1]Department of Neurology, BG Unfallkrankenhaus Berlin, Germany
[2]Department of Radiology and Neuroradiology, BG Unfallkrankenhaus Berlin, Germany
[3]Institute for Diagnostic Radiology and Neuroradiology, University Medicine Greifswald, Germany
[4]Center for Clinical Research, BG Klinikum Unfallkrankenhaus Berlin, Germany
[5]Department of Neurology, Charité Universitätsmedizin Berlin, Germany

Background & Purpose: Endovascular techniques for recanalization of large vessel occlusions (LVO) are being perfected constantly, meanwhile clinicians strive to optimize preclinical and clinical stroke protocols. In 2011 a Stroke Emergency Mobile (STEMO) was established in Berlin (Germany), enabling preclinical cranial computed tomographies (cCT) with angiography and preclinical i. v. thrombolysis.[1] Specialized neuroradiologies can be targeted in cases of LVO.[2] Studies proved that the STEMO reduces alarm-to-thrombolysis times significantly[3] and suggest that ultra-early i. v. thrombolysis might be associated with an improved functional outcome[4]. Subgroup analysis of patients with LVO have not been reported.

This study aims to analyze the effect of a STEMO on door-to-groin times in patients with LVO before thrombectomy.

Methods: Retrospective cohort-study of door-to-groin times in patients with LVO of the anterior circulation transported via STEMO and patients transported with conventional ambulances during 05/2017 und 12/2019.

Results: 140 patients were included in this analysis. 14 patients (10 %) where transported via STEMO. Mean age was 71.4 years (SD = 13.8) in the STEMO group and 73.1 years (SD = 14) in the non-STEMO group. Both groups included 50 % female and male patients. Mean door-to-groin time was significantly lower in the STEMO group (33.4 min, SD = 11.8 min vs. 89.3 min, SD = 39.3 min; $p < 0.001$, Fig. 1).

Conclusion: Introduction of a STEMO can reduce door-to-groin times in patients with LVO significantly. Further evaluation of this subgroup of patients is in progress to clarify weather neurological outcomes benefit from these preclinical processes as well.

References

1. Ebinger M, Rozanski M, Waldschmidt C, et al. PHANTOM-S: the prehospital acute neurological therapy and optimization of medical care in stroke patients-study. *Int J Stroke*. 2012;7(4):348–353. https://doi.org/10.1111/j.1747-4949.2011.00756.x
2. Nolte CH, Audebert HJ. Prähospitale Versorgung von Patienten mit Schlaganfall [Prehospital care for stroke patients]. *Med Klin Intensivmed Notfmed*. 2017;112(8):668–673. https://doi.org/10.1007/s00063-017-0348-z
3. Ebinger M, Winter B, Wendt M, et al. Effect of the use of ambulance-based thrombolysis on time to thrombolysis in acute ischemic stroke: a randomized clinical trial. *JAMA*. 2014;311(16):1622–1631. https://doi.org/10.1001/jama.2014.2850
4. Ebinger M, Kunz A, Wendt M, et al. Effects of golden hour thrombolysis: a Prehospital Acute Neurological Treatment and Opti-

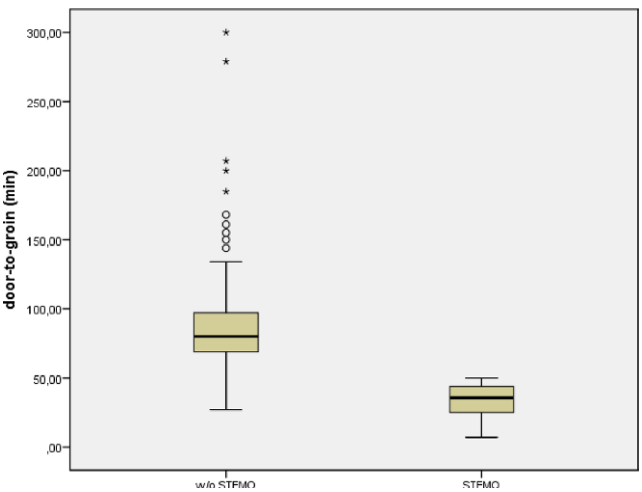

Fig. 1 Significantly reduced door-to-groin times in patients with LVO of the anterior circulation transported via STEMO (* $p < 0.001$)

mization of Medical Care in Stroke (PHANTOM-S) substudy. *JAMA Neurol*. 2015;72(1):25–30. https://doi.org/10.1001/jamaneurol.2014.

[31] Improving Brain Tumor Segmentation Through Candidate Segmentation Fusion

Lioba Grundl*[1], Florian Kofler[1,2], Tom Finck[1], Christoph Berger[2], Claus Zimmer[1], Björn Menze[2], Benedikt Wiestler[1]

[1]Dept. of Neuroradiology, TU Munich University Hospital, Munich, Germany
[2]Dept. of Informatics, TU Munich, Munich, Germany

Background & Purpose: Advances in Deep Learning have led to the development of segmentation algorithms which today rival human performance, as showcased in the BraTS challenge [1]. These algorithms clearly carry great scientific and clinical potential. Here, we evaluate BraTS Toolkit [2], designed to facilitate the use of state-of-the-art brain tumor segmentation.
Methods: We collected a total of 68 preoperative glioma MR exams (WHO Grades II–IV) from the TUM and REMBRANDT repositories. These were manually segmented and cross-validated by two neuroradiology residents into necrosis, contrast-enhancing tumor and edema. Cases were processed with BraTS Toolkit in a fully automated fashion and the resulting segmentations evaluated.
Results: All cases were successfully segmented. A majority voting fusion of the top 5 algorithms (Maj5; by BraTS performance) outperformed all single candidate segmentations for whole tumor segmentation both in Dice score and Hausdorff's distance (95th percentile) metrics (Fig. 1). This was corroborated when looking at structure segmentation (in particular edema and contrast-enhancing tumor). Also, false-positive detections were relevantly reduced in fusions.
Conclusion: Candidate segmentation fusions of BraTS algorithms relevantly improve single algorithm segmentation performance. In combination with BraTS Toolkit, objective glioma assessment by fully-automated segmentation is readily available for everybody. Future research will focus on improving fusions through Deep Learning or taking into account patch-wise semantic information.

References

1. Bakas et al., Identifying the Best Machine Learning Algorithms for Brain Tumor Segmentation, Progression Assessment, and Overall Survival Prediction in the BRATS Challenge. arXiv:1811.02629 (2019)
2. Kofler et al., BraTS Toolkit: Translating BraTS Brain Tumor Segmentation Algorithms Into Clinical and Scientific Practice. Frontiers in Neuroscience (2020)

[32] Radiation Exposure of Three Different CT Systems Used for Lumbar Puncture in Patients with Spinal Muscular Atrophy

Bronzlik P., Abu-Fares O., Lanfermann H., Götz F.

Institute for Diagnostic and Interventional Neuroradiology, Hannover Medical School, Hannover

Background and Purpose: Patients with spinal muscular atrophy (SMA) require repeated CT-guided lumbar puncture for cerebrospinal fluid analysis and intrathecal injection of nusinersen. We analysed the radiation exposure of 3 different CT systems used in our patients.
Methods: Retrospective evaluation of all CT-controlled lumbar punctures in patients with SMA since 11/2017. For each intervention, the number of scans as well as CTDI and DLP values were recorded separately for diagnostics and puncture.
Results: 110 CT-guided punctures, 59 on scanner A, 19 on B and 32 on C were successfully performed in 20 patients aged 11 to 65 years. The number of acquisitions per treatment was between 1 and 20, on average 4.7. With system C all cases were below the national diagnostic reference values (BfS) of the bony lumbar spine, they were exceeded with device A in 4/59 and B in 2/19 cases. The mean values of CTDI and DLP were 6.2 mGy-cm and 71.2 mGy-cm for diagnosis and 6.9 mGy-cm and 46.7 mGy for needle puncture, respectively. Interventional radiation exposure was lowest for CT-system C with CTDI and DLP values of 1.2 mGy-cm and 12.1 mGy.
Conclusion: The device performance contributes significantly to radiation exposure in CT-supported lumbar punctures of SMA patients. The radiation exposure of the most modern scanner is lower than the nation diagnostic reference values in all cases and results in the lowest amount of radiation exposure for needle-guidance.

[35] Differentiation of Lung Cancer Subtypes in Cerebral Metastases Using Apparent Diffusion Coefficient (ADC) Maps

Müller SJ Khadhraoui E, Riedel CH

Institute of Neuroradiology, University Medicine Göttingen

Background & Purpose: Brain metastases are common in patients with lung cancer. A non-invasive imaging biomarker with the ability to distinguish small cell lung cancer (SCLC) and non-small cell lung cancer (NSCLC) could accelerate the initiation of adequate therapy. Hypothetically, more cell membranes are found in solid tumor parts of

Fig. 1

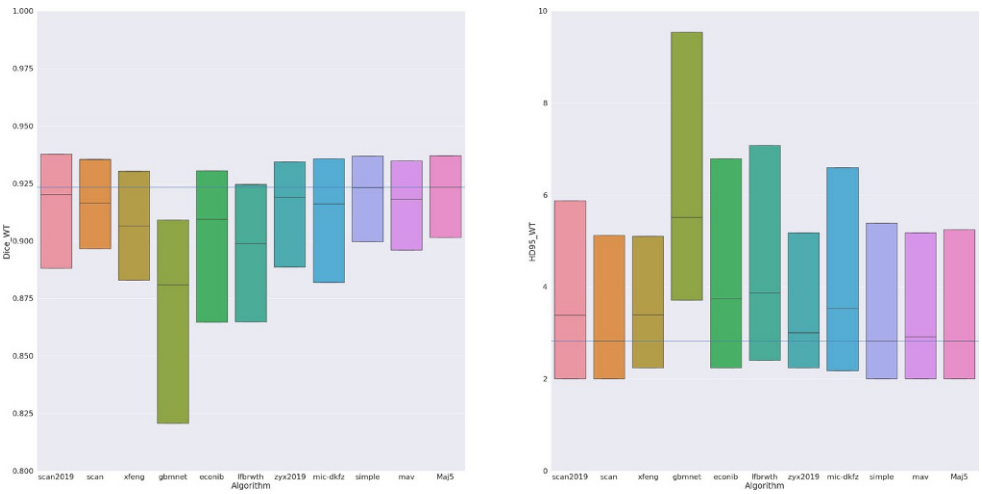

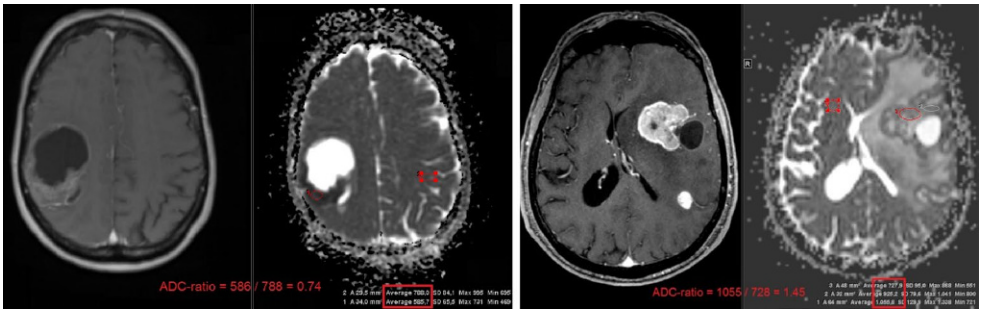

Fig. 1 Two examples of ADC-ratios of brain metastasis (T1 with CA and ADC map): *left*: typical SCLC, *right*: NSCLC

an SCLC than in NSCLC. Thus, the diffusion of water molecules might be more restricted in SCLS than in NSCLC. This study was undertaken with the aim of comparing ADC maps in SCLC and NSCLC.

Methods: We retrospectively analyzed 1500 cranial MR scans of 410 patients (298 NSCLC, 112 SCLC) from 2008 to 2019. The ADC-ratio was calculated by dividing the ADC value of the solid part of the metastasis by a reference value, which was measured in the ADC map using a symmetric position in the healthy contralateral hemisphere, as shown in Fig. 1.

Results: In 188 patients (54 with SCLC) brain metastases were detected. We included 65 pre-therapeutic patients (25 with SCLC) with histologically confirmed brain metastasis of lung cancer and an available pre-therapeutic MRI. In 100 % of the pre-therapeutic patients with SCLC the ADC value was significantly lower than the reference value, ADC-ratio(SCLC) was 0.69 ± 0.13 for the solid part of the metastasis. ADC-ratio(NSCLC) was 1.17 ± 0.36.

AR<0.9 (AR<0.8) shows a sensitivity of 100 % (76 %) and a specificity of 75 % (90 %) in detecting SCLC vs. NSCLC.

Conclusion: In pre-therapeutic patients with lung cancer and brain metastases with solid tumor parts, ADC-ratio enables a good differentiation of SCLC and NSCLC.

[36] MRSI Detectable Choline Metabolism as Marker for Gender Differences in Aging

Pilatus U, Wachter L, Ludin N, Matura S, Silaidos C, Pantel J, Eckert GP, Hattingen E

Institut für Neuroradiologie, Klinik für Allgemeinmedizin und Brain-Imaging-Center, Goethe-Universität Frankfurt
Institut für Ernährungswissenschaften, Justus-Liebig-Universität Gießen

Background & Purpose: Cerebral phospholipid membranes are involved in signaling functions and cell aging processes. Estrogens can influence the fluidity and function of membrane phospholipid layers. In vivo 1H/31P MR-spectroscopic imaging (MRSI) of the brain allows quantifying different compounds of the membrane lipid metabolism to investigate sex- and/or age-related differences in healthy subjects.

Methods: ^{1}H-MRSI and ^{31}P-MRSI was acquired in 130 healthy volunteers (33 young females, 35 old females, 32 young males, 30 old males; mean age 26.58 ± 0.5 (young) and 70.92 ± 1.0 (old)). Data were analyzed from the target regions (Fig. 1). According to [1] the sum of 31P-MRS detectable Cho-containing compounds (PCho+GPC) will amount to 1.6 mMol/l while tCho obtained from 1H-MRS will be 1.9 mMol/l. Based on this assumption, bars scaled to the averaged signal intensity for each modality are shown in Fig. 2.

Results: MRSI revealed lower tCho in young women compared to men and to older women ($p<0.01$ for GM, WM). Phosphorylated PCho and GPC were not significantly different between the groups ($p=0.45$ for WM, $p=0.06$ for GM). In general, the sum of PCho and GPC was less than the tCho concentration hinting to a residual choline fraction (rCho) invisible with 31P-MRSI. This fraction was lower in young females ($p<0.01$ for GM; WM) and it may account for the lower tCho concentration.

Conclusion: Increased rCho may be attributed to increased lipid mobility [1]. Thus, lower rCho levels may indicate higher integrity of cerebral membrane phospholipids of young females. A possible reason is the higher estrogen level in young females.

References

1. Hattingen et al., Combined 1H and 31P spectroscopy provides new insights into the pathobiochemistry of brain damage in multiple sclerosis; *NMR Biomed.* 2011; 24: 536–546.

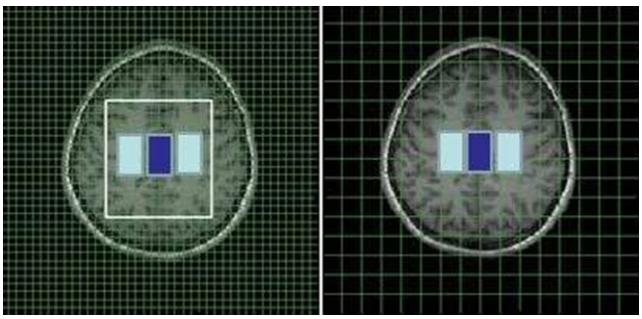

Fig. 1 Target regions: light blue WM, dark blue GM; the grid shows the spatial resolution for each modality, left panel 1H-MRSI, right panel 31P-MRSI

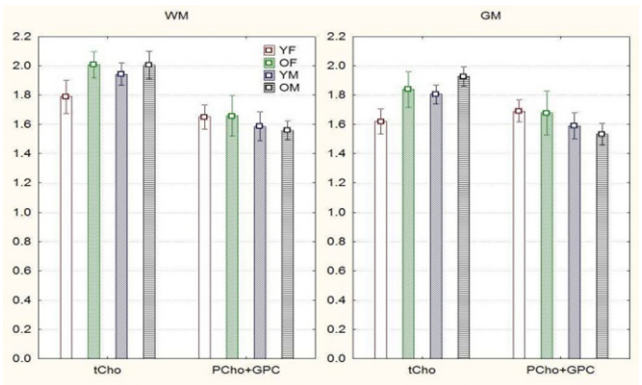

Fig. 2 Choline concentrations (institutional units adapted to mMol/l) in WM and GM for young females (YM), old females (OF), young males (YM) and old males (OM). The left part of each panel shows 1H-MRS data (tCho), while the left part shows 31P-MRS data (PCho+GPC)

[37] mdbrain–DeepVol vs. FreeSurfer: Repeatability and Performance Measurements in Brain Volumetry

H. Michaely[1], P.F. Bertran[2], J. Opalka[2], A. Lemke[2] and P. Mann[2]

[1]MVZ Radiologie Karlsruhe
[2]mediaire GmbH, Berlin

Background & Purpose: To test and compare repeatability and diagnostic accuracy of brain volumetry using md**brain**'s DeepVol and FreeSurfer
Methods: Brain volumetry was carried out with FreeSurfer and compared to DeepVol. Both algorithms were tested on the MIRIAD* data set (45 patients with confirmed Alzheimer's disease (age 69.4 y+/–7.1 y) and 23 healthy controls (age 69.7 y+/–7.2 y) scanned over a course of 2 y including two back-to-back scans ($n=178$)). Images were acquired on a 1.5 T MR-scanner using 3D-T1w images. Volumetry was performed for: whole brain, grey&white matter, frontal, parietal, occipital, temporal lobe, hippocampus and ventricles. Both algorithms were compared in terms of (a) repeatability, (b) performance and (c) sensitivity/specificity. For (a) only the back-to-back scans were used. (b) Performance was tested with respect to the algorithm's ability to correctly identify healthy patients and those with confirmed Alzheimer's. For that, ROC was used to calculate the corresponding AUC, and (c) sensitivity/specificity on the best performing regions.
Results: For (a), DeepVol showed a significantly higher stability (mean deviations of 0.25 % vs. 1.03 %). Performance analysis yielded higher AUC value of up to 0.96 for the Hippocampus compared to 0.94. Additionally, slightly increased sensitivity/specificity of 0.96/0.98 for DeepVol as compared to 0.93/0.96 were calculated when both hippocampus and temporal lobe were taken into account.
Conclusion: DeepVol shows better results for (a)–(c) independent of the evaluated regions. This is reflected by the improved mean values and a decreased error. Taking into account the shorter evaluation time of ~3 min vs. ~10 h, DeepVol appears to be a valuable tool for a daily application in clinical practice.

References

1. https://www.ucl.ac.uk/drc/research/methods/minimal-interval-resonance-imaging-alzheimers-disease-miriad

[38] Comparison of the Diffusion-Weighted STEAM-DWI and the EPI-DWI in Ischemic Stroke

Müller SJ[1], Khadhraoui E[1], Voit D[2], Riedel CH[1], Frahm J[2]

[1]Institute of Neuroradiology, University of Göttingen
[2]Max Planck Institute for Biophysical Chemistry, Göttingen

Background & Purpose: Diffusion-weighted imaging in stimulated echo detection mode (STEAM-DWI) is an interesting alternative compared to the most commonly used diffusion-weighted echo-planar imaging (EPI-DWI). A novel STEAM-DWI, described by Merrem et al. 2017, was routinely performed together with the "gold standard" EPI-DWI (See Fig. 1 for an example).
Methods: EPI- and STEAM-DWIs with 3 mm layer thicknesses were performed between 01 July 2019 and 30 June 2020 by means of 3-T MRI in patients with suspected subacute stroke. Three neuroradiologists independently and separately assessed both the EPI- and the STEAM-DWI, stating (i) whether there was a stroke, (ii) which vessel it was associated with, (iii) the presence of artifacts and (iv) whether it was infra- or supratentorial. In case of an embolic shower, the count of impacts should be detected. The sensitivity and specificity of the STEAM-DWI compared to the EPI-DWI for detecting a stroke was determined.
Results: In 53 (23 right, 21 left, 9 both hemispheres) of 85 patients a subacute stroke was confirmed using the EPI-DWI. The following territories were mainly affected: ACA 8 %, MCA 45 %, PCA 27 %, Brainstem 10 %, Cerebellum 10 %. In 51/53 cases the STEAM-DWI detected a stroke (96.2 %), in 35 of 37 patients microembolic events were noticed (94.6 %). Results show a sensitivity and specificity of 100 % (74/74) for major infarcts (>4 mm² in-plan) and a sensititvity of 90.5 % (124/137) and specificity of 100 % for detecting subacute microembolic lesions. Less artifacts were noticed in the STEAM DWI.
Conclusion: STEAM DWI can be used for diagnosis of subacute strokes and could provide additional information, especially in cases with a high level of susceptibility artifacts.

References

1. Merrem, A. et al.: Rapid diffusion-weighted MRI of the brain without susceptibility artifacts: Single-shot STEAM with radial undersampling and iterative reconstruction. Invest Radiol 52, 428–433 (2017), https://doi.org/10.1097/RLI.0000000000000357

[39] Distal Intracranial Thrombectomy with Tigertriever 13

Nordmeyer H[1], Fischer S[2], Will L[2], Phung T[1], Weber W[2]

[1]radprax Neurocenter Solingen, Dept. of interventional Radiology and Neuroradiology
[2]Hospital Knappschaft Bochum, Dept. of diagnostic and interventional Radiology and Neuroradiology

Background & Purpose: Mechanical recanalization of acute intracranial occlusions of the anterior and posterior cerebral artery and middle cerebral artery segments distal to M2 remains a matter of debate. Embolisms to new territories (ENT) occur in up to 4–9 % according to

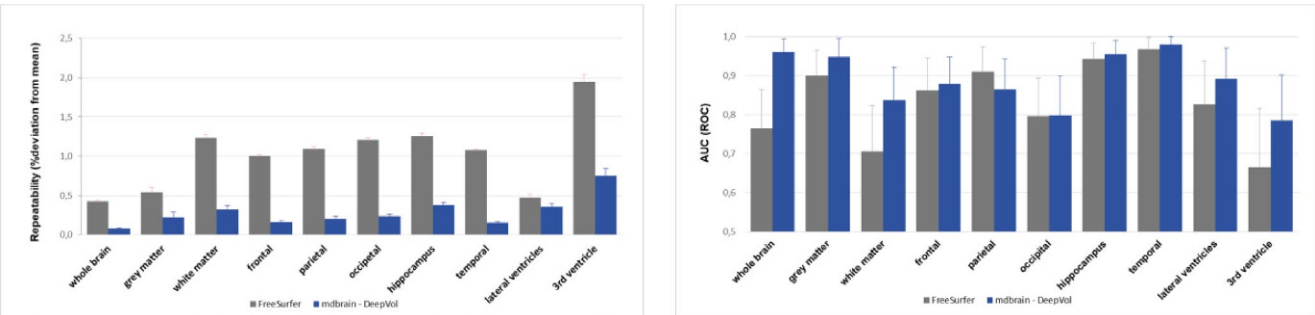

Fig. 1 **a** Reproducibility and **b** performance tests of brain volumetry (mean +/– CI95) carried out on the MIRIAD* MR datasets using mdbrain–DeepVol (*blue*) and FreeSurfer (*grey*). The error bars show the variability using the backto back scans for **a** whereas for **b** error bars are based on recalculating the AUC multiple times by sampling with replacement over the used dataset. mdbrain–DeepVol showed significantly higher repeatability over all regions ($p<0.05$). A higher performance was also calculated, although not statistically significant

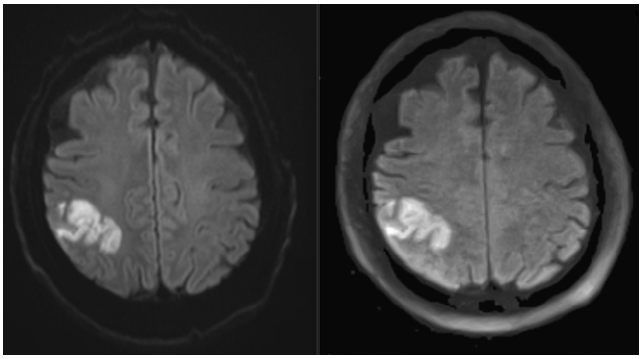

Fig. 1 B1000 of EPI- (*left*) and STEAM-DWI (*right*), both show a subacute infarction

randomized prospective trials where distal embolisms in the territory of the primarily occluded vessel are not even included as they usually are not detected until the target vessel is recanalized. Navigation and retrieval maneuvers in distal segments may lead to higher rates of intracranial hemorrhage. Due to the clinical relevance of distal embolism to eloquent brain areas, an atraumatic and efficient system is required.
Purpose: To report the experience with the Tiger 13 as an adjustable clot retriever with a low crossing profile that allows distal navigation through a 0.013" microcatheter.
Methods: Distal thrombectomy with the Tiger 13 was performed in either primarily or secondarily occluded vessels that were ineligible for the use of regular stentretrievers.
Results: From 2019 to 2020 43 patients from two neurovascular centers were included. 50 occlusions in M2, M3, A2, A3 and distal PCA segments were treated with Tiger 13. In 37 occlusions Tiger13 was used for recanalization of the initial occlusion or for ENT (intention-to-treat group). In 9 occlusions Tiger13 was used as a bail-out device. Successful recanalization (TICI 2b–3) was achieved in 94 %.

Intracranial hemorrhage (SAH or ICH) occurred in 6 patients where none of those were classified as symptomatic.
Conclusion: Tiger 13 together with a 0.013" microcatheter is safe and effective and allows for atraumatic navigation in distal occlusions of the anterior and posterior circulation.

[40] Cerebral Blood Volume (CBV) Index as an Indicator of Collateral Capacity is Associated with Clinical Outcome After Endovascular Therapy in Acute Ischemic Stroke

Dominik Sepp[1], Claus Zimmer[1], Maria Berndt[1], Sebastian Mönch[1], Silke Wunderlich[2], Benjamin Friedrich[1], Tobias Boeckh-Behrens[1], Christian Maegerlein[1]

[1]Department of Diagnostic and Interventional Neuroradiology, Klinikum rechts der Isar, Technical University of Munich, Germany
[2]Department of Neurology, Klinikum rechts der Isar, Technical University of Munich, Germany

Background & Purpose: Endovascular therapy of acute ischemic stroke has proven highly effective in selected patients. But the patients' selection criteria are still under discussion. Collateral flow is known to be an important factor, but its evaluation is often subjective and time-consuming. CBV index is a presumed indicator of collateral capacity and can be provided fast and easily by automated quantitative analysis.

We evaluated in this study the relationship of the CBV index from the affected region with the clinical outcome in acute ischemic stroke patients after endovascular therapy.
Methods: We included consecutive patients admitted to our hospital with acute ischemic stroke of the anterior circulation treated with endovascular therapy. CBV index was automatically analyzed by RAPID software by dividing the average of CBV from the affected region (Tmax<6 s) by normal CBV.
Results: 155 patients were included in this study. The rate of successful recanalization (TICI≥2b) was 89.1 %. 66 patients (42.58 %) had a good clinical outcome (90-day mRS ≤2) and a significant improvement of the NIHSS. Median CBV index was 0.7 ± 0.16. Higher CBV index was associated with good clinical outcome ($p < 0.001$) and with significant NIHSS improvement ($p = 0.001$) also after adjustment for NIHSS at baseline, age and Aspect-score ($p = 0.005$; $p = 0.009$).
Conclusion: Higher CBV index at baseline is associated with good clinical outcome in patients with acute ischemic stroke after endovascular therapy. CBV index is a presumed indicator for collateral capacity that can be obtained fast and automatically using CT-Perfusion imaging. This could improve current selection criteria for endovascular treatment especially in complex cases.

[43] Mechanical Thrombectomy in Stroke Patients with Acute Occlusion of the M1-Compared to the M2-segment: Safety, Efficacy and Clinical Outcome

Daniel Weiss[1], Christian Rubbert[1], Vivien Lorena Ivan[1], John-Ih Lee[2], Michael Gliem[2], Sebastian Jander[2], Julian Caspers[1], Bernd Turowski[1], Marius Kaschner[1]

[1]Department of Diagnostic and Interventional Radiology, University Düsseldorf, Medical Faculty, Düsseldorf, Germany
[2]Department of Neurology, University Düsseldorf, Medical Faculty, Düsseldorf, Germany

Purpose: Endovascular treatment (ET) in occlusions of the M1- and proximal M2-segment of the middle cerebral artery (MCA) is an established procedure. In contrast, ET in distal M2-occlusions has not yet been sufficiently evaluated (1–2). The purpose of this study was to assess relevant parameters for clinical outcome, efficacy and safety of patients undergoing ET in M1-, proximal M2- and distal M2-occlusions.
Methods: One-hundred-seventy-four patients undergoing ET in acute ischemic stroke with an occlusion of the M1- or M2-segment of the MCA were prospectively enrolled (a-priori power-analysis showed power = 75 % for a moderate effect-size). Group comparisons in three-months modified Rankin Scale (mRS), TICI scale and NIHSS were performed. Binary-logistic-regression-models were calculated for each occlusion site concluding age, NIHSS at admission, Maas Score, onset-to-recanalization-time and complication rate as independent variables and dichotomized three-months mRS as dependent variable.
Results: There were no significant group differences in three-months mRS, TICI scale or complication rates between M1- and M2-occlusions nor between proximal and distal M2-occlusions. Binary-logistic-regression in patients with M1-occlusions showed a substantiate explanation of variance ($NR^2 = 0.35$) of mRS and significantly contributing factors were NIHSS ($p = 0.009$) and Maas Score ($p = 0.01$). Binary-logistic-regression in M2-occlusions showed a high explanation of variance ($NR^2 = 0.50$) of mRS but no significant results.
Conclusions: Clinical outcome and procedural safety of patients with M2-occlusions undergoing ET are comparable to those of patients with M1-occlusions. Clinical outcome of patients with M1-occlusions undergoing ET is primarily influenced by the initial neurological deficit and the collateralization of the occlusions. By contrast, clinical outcome in patients with M2-occlusions is more multifactorial.

References

1. Salahuddin, H., et al., *Mechanical thrombectomy of M1 and M2 middle cerebral artery occlusions.* J Neurointerv Surg, 2018. **10**(4): p. 330–334.
2. Ivan, V.L., et al., *Mechanical thrombectomy in acute middle cerebral artery M2 segment occlusion with regard to vessel involvement.* Neurol Sci, 2020.

[45] Deep Learning Segmentation for 3D Intracranial Aneurysm Models

Annika Niemann[1,2], Lisa Schneider[1], Belal Neyazi[3], Oliver Beuing[4], Philipp Berg[2,5], Sylvia Saalfeld[1,2], Naomi Larsen[6]

[1]Institut für Simulation und Graphik, Otto-von-Guericke Universität Magdeburg, Magdeburg, Germany
[2]Forschungscampus *STIMULATE*, Otto-von-Guericke Universität Magdeburg, Magdeburg, Germany
[3]Universitätsklinik für Neurochirurgie, Universitätsklinikum Magdeburg, Magdeburg, Germany
[4]AMEOS Klinikum Bernburg, Bernburg, Germany
[5]Institut für Strömungstechnik und Thermodynamik, Otto-von-Guericke Universität Magdeburg, Magdeburg, Germany
[6]Klinik für Radiologie und Neuroradiologie, Universitätsklinikum Schleswig-Holstein Campus Kiel, Kiel, Germany

Background: Intracranial aneurysm analysis is often supported by measuring several morphological parameters, for example aneurysm width, height and aspect ratio. These parameters are based on the geometry of the aneurysm sac, the aneurysm neck and the parent vessel. To allow fast, consistent and exact measurements, they should be calculated automatically in 3D. Prior to morphological analysis, segmentation of the aneurysm is required.
Methods: We present a deep learning segmentation of 3D models of intracranial aneurysms. This detailed deep learning segmentation is trained to detect not only the aneurysm, but also segments the surrounding structures in vessels and bifurcations. Additionally the inlet vessel is segmented.

Based on the segmentation an abstract graph representation of the aneurysm is generated and allows identification of the parent vessel and vessels which arise directly at the aneurysm. The program was trained with aneurysms from four different institutions.

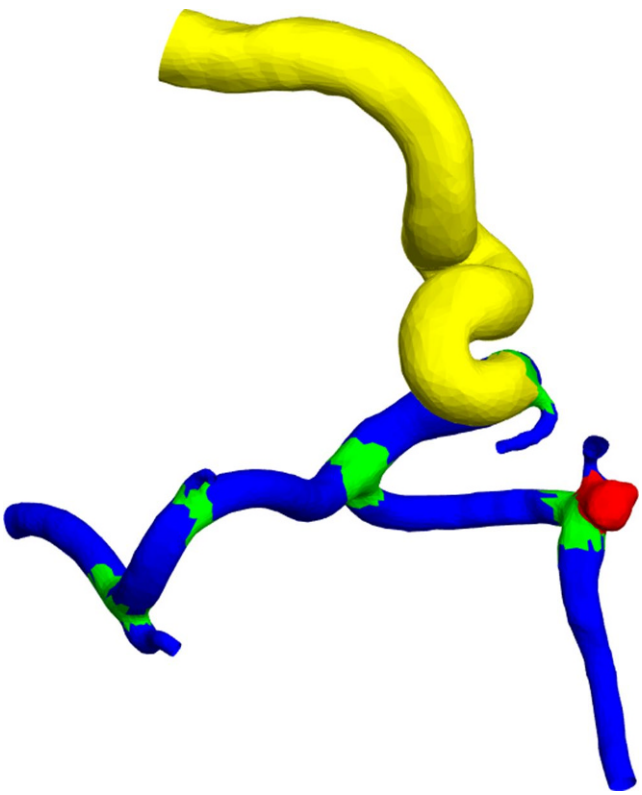

Fig. 1

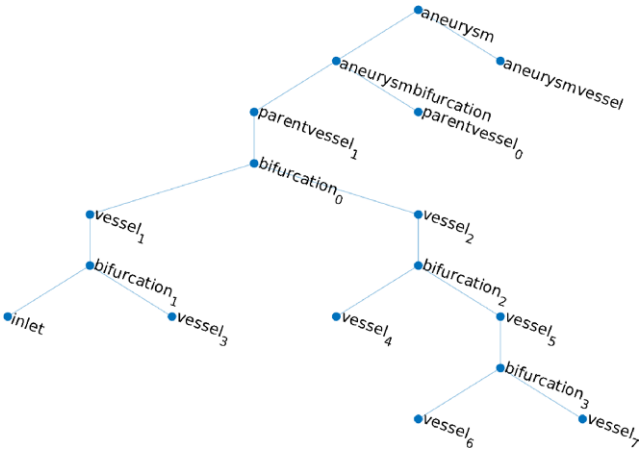

Fig. 2

Results: The presented algorithm segments the aneurysm and the surrounding vessels. The best segmentation results are achieved for the aneurysm and the inlet vessel.
Conclusions: The combination of automatic segmentation in multiple parts and semantic analysis provide a useful basis for further analysis and calculation on intracranial aneurysms.

[46] Opportunistic QCT Bone Mineral Density Measurements Predicting Osteoporotic Fractures: A Use Case in a Prospective Clinical Cohort

Yannik Leonhardt[1], Pauline May[2], Olga Gordijenko[3], Veronika Koeppen[4], Henrike Brandhorst[2], Claus Zimmer[5], Marcus R. Makowski[1], Thomas Baum[5], Jan S. Kirschke[5], Alexandra S. Gersing[1], Vanadin Seifert-Klauss[2], Benedikt J. Schwaiger[5]

[1]Department of Radiology, School of Medicine, Technical University of Munich, Germany
[2]Department of Gynaecology, School of Medicine, Technical University of Munich, Germany
[3]Department of Trauma Surgery, School of Medicine, Technical University of Munich, Germany
[4]Department of Orthopedics and Sports Orthopedics, School of Medicine, Technical University of Munich, Germany
[5]Department of Neuroradiology, School of Medicine, Technical University of Munich, Germany

Purpose: To assess whether volumetric vertebral bone mineral density (BMD) measured with opportunistic QCT (i.e., CT acquired for other reasons) can predict osteoporotic fracture occurrence in a prospective clinical cohort.
Methods: In the database of our fracture liaison service, 58 patients (73 ± 11 years, 73 % women) were identified that had at least one prevalent fracture clinically assumed to be osteoporotic and had undergone CT. BMD was determined by converting HU using scanner-specific conversion equations. Baseline DXA was available for 31 patients. During a 3-year follow-up, new fractures were diagnosed either by (i) recent in-house imaging or (ii) clinical follow-up with validated external reports. Associations were assessed using logistic regression models, and cut-off values were determined with ROC/Youden analyses.
Results: Within 3 years, 21 of 58 patients presented an incidental vertebral fracture (36 %). Mean BMD and age of patients with fractures were significantly lower (56 ± 20 vs. 91 ± 38 mg/cm^3; 77 ± 10 vs. 71 ± 11 years). QCT BMD was significantly associated with the occurrence of new fractures ($p = 0.005$, OR = 1.034 per BMD unit decrease; 95 % CI, 1.010–1.058). For the differentiation of patients with and without incidental fractures, ROC showed an AUC of 0.76 and a Youd-

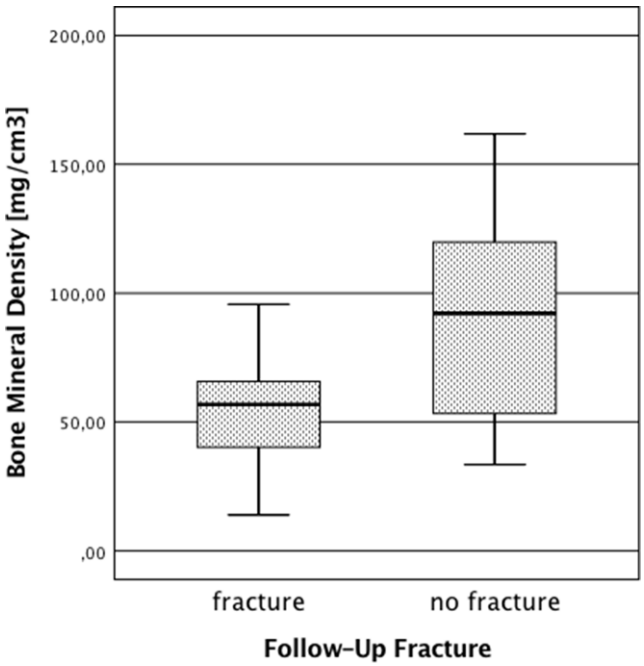

Fig. 1 Bone mineral density in patients with and without follow-up fracture. The BMD was calculated using the initial baseline CT scans

en's Index of J = 0.48, suggesting an optimal cut-off value of 82 mg/cm^3. In contrast, DXA T-scores showed no significant association with incidental fractures in analogous regression models.
Conclusion: In this use case, opportunistic BMD measurements predicted incidental vertebral fractures during a 3-year follow-up. This suggests that opportunistic measurements are useful to reduce the diagnostic gap and evaluate the fracture risk in osteoporotic patients.

[48] Applications of DWI-based Fiber Tractography: Connectivity Fingerprints of Adverse Effect Provoking Contacts in Parkinson's Deep Brain Stimulation

Strotzer Q[1], Anthofer J[1], Beer A[2], Fellner C[3], Schlaier J[1]

[1]Department of Neurosurgery, University Hospital Regensburg, Germany
[2]Department of Psychology, University of Regensburg, Germany
[3]Department of Radiology, University Hospital Regensburg, Germany

Background & Purpose: To improve target planning in deep brain stimulation for Parkinson's disease, we investigated which cortical and subcortical structures are involved in the occurrence of side-effects using fiber tractography based on diffusion-weighted imaging.
Methods: Twenty-one Parkinson's patients with bilateral subthalamic deep brain stimulation were examined. For each of the 168 electrode-contacts (four contacts per hemisphere), the connectivity to specific cortical and subcortical structures was assessed using probabilistic tractography based on diffusion-weighted magnetic resonance imaging (64 gradient directions). Motor and oculomotor side-effects, paresthesia, dysarthria, hyperkinesia, and other complications were separately assessed for every electrode-contact during the initial programming session. The contacts were categorized into groups of side-effect provoking and non-provoking contacts. Finally, these groups were compared for their connectivity-patterns.
Results: We found significant ($p < 0.05$) differences in the connectivity of contacts that provoked certain side-effects compared to contacts that were non-provoking. Especially paresthesia and dysarthria provoking contacts were significantly more often than non-provoking contacts connected to distinct cortical areas like the supplementary motor area, fibers of the internal capsule, and structures of the basal ganglia-thalamo-cortical circuitry. Connectivity-patterns differed for the different adverse effects.
Conclusion: Certain side-effects of subthalamic deep brain stimulation seem to be associated with electrode-contacts maintaining specific connectivity-patterns. We conclude that considering a symptom-specific and connectivity-based approach may improve the outcome of deep brain stimulation for Parkinson's disease by helping to achieve more individual targeting in deep brain stimulation surgery.

[49] Diagnostic Accuracy Of Optimized Reconstruction on Dual-Layer Spectral CT for the Detection of Posttraumatic Prevertebral Hematoma of the Cervical Spine

Sedaghat S, Langguth P, Larsen N, Both M, Jansen O

University Hospital Schleswig-Holstein Campus Kiel, Department for Radiology and Neuroradiology

Background & Purpose: The aim of this study was to investigate the diagnostic value of dual-layer spectral detector computed tomography (SDCT) in the detection of posttraumatic prevertebral hematoma of the cervical spine by using optimized imaging reconstructions.
Methods: 38 patients with posttraumatic imaging of the cervical spine were included and underwent both SDCT and MRI. MRI was set as reference and combined conventional/electron density (C + ED) images were compared to conventional CT (CCT) images. Images were evaluated by two blinded readers.
Results: 18 prevertebral hematomas were identified. The mean age of the patients was 63 ± 22.9 years. Reader 1 identified 14 of 18 and reader 2 15 of 18 prevertebral hematomas by using C + ED reconstructions. 6 of 18 and 9 of 18 hematomas were seen on CCT by reader 1 and 2, respectively. CCT showed a sensitivity of 33–50 % and a specificity of 75–80 %, while C + ED reconstructed images had a sensitivity of 77–83 % and a specificity of 85–90 %. Accuracy increased from 55–66 % to 84 % by using C + ED images. The minimum thickness for the detection of hematoma on C + ED images was 3 mm. Readers showed an excellent inter-rater reliability (kappa = 0.82) for C + ED images and a moderate inter-rater reliability (kappa = 0.44) for CCT.
Conclusion: SDCT allows an increased accuracy for the detection of posttraumatic prevertebral by using combined conventional and electron density reconstructions, compared to conventional images.

[50] Radiological Follow-up of Cerebral Arteries after Treatment with Compliant and Non-Compliant Balloons for Cerebral Vasospasm Following Subarachnoid Hemorrhage

Alexander Neumann[1], Jan Küchler[2], Claudia Ditz[2], Kara Krajewski[2], Jan Leppert[2], Peter Schramm[1], Hannes Schacht[1]

[1]Department of Neuroradiology, University Medical Center Schleswig-Holstein, Campus Lübeck, Germany
[2]Department of Neurosurgery, University Medical Center Schleswig-Holstein, Campus Lübeck, Germany

Background & Purpose: Treatment of cerebral vasospasm after subarachnoid hemorrhage with compliant and non-compliant balloon catheters remains controversial since it bears in principle the risk for devastating acute complications with both balloon types having different mechanical properties, which can lead to vessel injury. As a late complication, high grade stenoses have been reported sporadically [1, 2]. We analyzed the radiological follow-up of vasospastic cerebral arteries treated with different balloon types to obtain data about the incidence and relevance of long-term vessel changes [3].
Methods: We retrospectively analyzed 30 arterial vessel segments treated with compliant ($n = 23$) and non-compliant ($n = 7$) balloons for cerebral vasospasm after subarachnoid hemorrhage concerning radio-

logical follow-up as well as patients' clinical characteristics and functional outcome after 3 months.
Results: Only mild delayed vessel narrowing was detected in 13 % of balloon treated vessels with no evident differences between both balloon types. Moderate or high grade late occurring stenoses were not observed after treatment with compliant or non-compliant balloons.
Conclusion: Our data support transluminal balloon angioplasty as a safe treatment option for cerebral vasospasm concerning long-term complications with no differences between compliant and non-compliant balloons.

References

1. Sedat J et al., Restenosis after balloon angioplasty for cerebral vasospasm, J Cardiovasc Intervent Radiol 2009; 32: 337–40.
2. Safain MG et al., Delayed progressive bilateral supraclinoid internal carotid artery stenosis in a patient with a ruptured basilar artery aneurysm, J Clin Neurosci 2015; 22: 368–72.
3. Neumann A et al., Non-Compliant and Compliant Balloons for Endovascular Rescue Therapy of Cerebral Vasospasm after Spontaneous Subarachnoid Hemorrhage: Experiences of a Single Center Institution with Radiological Follow-up of the Treated Vessel Segments, Stroke Vasc Neurol; accepted for publication on June 24, 2020.

[52] Machine Learning to Support Interventionalist in Patient Selection for Endovascular Thrombectomy: Early Identification of Cases with Dismal Outcome at Discharge

Máté E. Maros[1,2], Tabea Gerdes[1], Chang Gyu Cho[1], Victor Saase[1], Benedikt Kämpgen[6], Fabian A. Flottmann[5], Eva Neumaier-Probst[1], Mansour Alzghloul[1], Alex Förster[1], Angelika Alanso[4], Michael Platten[4], Thomas Ganslandt[2], Michael Neumaier[3], Christoph Groden[1], Holger Wenz[1]

[1]Department of Neuroradiology, Medical Faculty Mannheim, Heidelberg University, Mannheim, Germany
[2]Department of Biomedical Informatics at the Heinrich-Lanz-Center, Medical Faculty Mannheim, Heidelberg University, Mannheim, Germany
[3]Institute for Clinical Chemistry, Medical Faculty Mannheim, Heidelberg University, Mannheim, Germany.
[4]Clinic for Neurology, Medical Faculty Mannheim, Heidelberg University, Mannheim, Germany
[5]Department of Diagnostic and Interventional Neuroradiology, University Medical Center Hamburg-Eppendorf, Hamburg, Germany
[6]Empolis Information Management GmbH, Kaiserslautern, Germany

Background & Purpose: Patient selection for endovascular thrombectomy (EVT) is still a challenging task for neuroradiologists. Identifying patients at the earliest stage of presentation that might benefit the most from by EVT or *vica versa* is an imperative[1]. Here, we investigated whether machine learning (ML) workflows can support interventionalists in patient selection based on early-phase clinico-radiological and laboratory data by predicting poor outcome[2].
Methods: A single-center retrospective cohort of 172 (90 M; 52.3 %) consecutive patients undergoing EVT in 2017–2018 was retrieved from local RIS/PACS. Admission ASPECTS was extracted from reports using NLP[3] and re-evaluated by two blinded readers on imaging. Explanatory variables included age, sex, comorbidities and blood rheology parameters as well as neuro-interventional procedural data on time, retrieval count and final Thrombolysis in Cerebral Infarction following angiography. The primary outcome was the modified Rankin Scale (mRS) score at hospital discharge. Poor outcome was defined as mRS 5–6 (98; 56.9 %). Previously described multistage 5-fold cross-validated ML-workflows using random forests (RF) were applied to subsets of the features available at pre- and post-EVT[2].
Results: All pre- and post-EVT features were available for 140 cases. Eighty-five cases (60.7 %) had poor outcome. The pre-EVT-RF model showed an accuracy of 65 % while the post-EVT-RF model achieved slightly higher performance of 67.9 %.
Conclusion: ML-supported patient selection for optimized EVT outcome is feasible, however, this is a hard task at the earliest stage of diagnosis even when considering several clinico-radiological and laboratory parameters.

References

1. Nishi, Hidehisa, et al. "Predicting clinical outcomes of large vessel occlusion before mechanical thrombectomy using machine learning." Stroke 50.9 (2019): 2379–2388.
2. Maros, Máté E., et al. "Machine learning workflows to estimate class probabilities for precision cancer diagnostics on DNA methylation microarray data." Nature protocols 15.2 (2020): 479–512.
3. Maros, Máté E., et al. "Comparative analysis of machine learning algorithms for computer-assisted reporting based on fully automated cross-lingual RadLex® mappings." Preprints (2020).

[53] Mechanical Thombectomy in Acute Ischemic Stroke Using a Manually Expandable Stenttriever (Tigertriever): Preliminary Single-Center Experience

L. Will[1], V. Maus[1], C Maurer[2], A. Weber[1], W. Weber[1], S. Fischer[1]

[1]Knappschaftskrankenhaus Bochum-Langendreer-Universitätsklinik-Institut für diagnostische und Interventionelle Radiologie, Neuroradiologie, Nuklearmedizin, Bochum, Germany
[2]Universitätsklinikum Augsburg, Klinik für Diagnostische Radiologie und Neuroradiologie, Augsburg, Germany

Objective: The aim of this study was to evaluate the safety and efficacy of a manually expandable stenttriever (Tigertriever, Rapid Medical, Yoqneam, Israel) in the treatment of acute ischemic stroke caused by intracranial large vessel occlusions (LVO).
Methods: We performed a single center retrospective analysis of all patients treated by mechanical thrombectomy due to LVO using the Tigertriever solely or in combination with other thrombectomy devices. The angiographic and clinical success was evaluated by the modified thrombolysis in cerebral infarction score (mTICI) and the modified Rankin score (mRS).
Results: 68 acute intracranial arterial occlusions in 61 patients (42 female, median age 77, range 43–92 years) were treated by mechanical thrombectomy using the Tigertriever. The successful reperfusion rate (mTICI 2b–3) was 85.3 % (58/68 procedures) with a first past effect (mTICI 3) of 23.5 % (16/68 occlusions). In the 46 cases carried out with the Tigertriever alone (absence of other thrombectomy devices) the success rate was 91.3 % (42/46 occlusions) with a first pass effect (mTICI 3) of 34.8 % (16/46 occlusions). In seven patients a mild subarachnoid hemorrhage occurred (11.5 %). None of these patients experienced a clinical sequel. At discharge, 39.3 % of the patients (24/61) had a favourable clinical outcome (mRS 0–2).
Conclusion: The Tigertriever offers a safe and effective treatment option for intracranial LVOs with promising reperfusion and low complication rates comparable to other stenttriever devices. Further comparative trials will help to prove the value of the Tigertriever among the existing technologies for mechanical thrombectomy.

[54] WEB for Atypical Aneurysm Locations

S. Zimmer[1], V. Maus[1], C. Maurer[2], A. Berlis[2], W. Weber[1], S. Fischer[1]

[1]Knappschaftskrankenhaus Bochum-Langendreer-Universitätsklinik-Institut für diagnostische und Interventionelle Radiologie, Neuroradiologie, Nuklearmedizin, Bochum, Germany
[2]Universitätsklinikum Augsburg, Klinik für Diagnostische Radiologie und Neuroradiologie, Augsburg, Germany

Background: The safety and efficacy of the Woven Endobridge Device (WEB) has been shown in multiple good clinical practice (GCP) trials, whereas aneurysm locations in these trials were restricted to bifurcation aneurysms located at the circle of Willis (MCA bif, ICA bif, A com A, BA tip).
Objective: To evaluate angiographic and clinical results with the WEB 17 in aneurysm locations that were excluded from the GCP trials, assuming that the angiographic and clinical results are similar to those of the GCP trials for aneurysms in traditional locations.
Methods: Retrospective analysis of immediate and follow-up results of aneurysms in locations outside the GCP trials were the WEB 17 was applied on an intention-to-treat approach.
Results: Between June 2017 and May 2020 47 aneurysms in 44 patients meet the inclusion criteria. Aneurysm locations were the ICA P com in 19 (40.3 %), ICA paraophthalmic or choroidal in 4 (8.6 %), ACA A2 segment in 12 (27.7 %), MCA M1 segment in 2 (4.3 %), PCA P2 segment in 2 (4.3 %), PICA in 3 (6.4 %) and the superior cerebellar artery in 4 (8.4 %) cases. The procedure related morbidity and mortality in the entire series was 0.0 %. The complete occlusion rate at 3 and 12 months was 63.9 % (23/36) and 75.0 % (15/20).
Conclusion: The WEB 17 is safe and effective in aneurysm locations different from the traditional bifurcation aneurysms included in the GCP trials. Further studies will help to define the entire spectrum of aneurysm morphologies and locations suitable for the WEB 17.

[55] Initial Experience with Surpass Evolve Flow Diverter in the Treatment of Intracranial Aneurysms

Maus V[1], Weber W[1], Berlis A[2], Maurer C[2], Fischer S[1]

[1]Department of Diagnostic and Interventional Neuroradiology and Nuclear Medicine, Ruhr University, Knappschaftskrankenhaus Bochum, Bochum, Germany
[2]Department of Diagnostic and Interventional Neuroradiology, University Hospital Augsburg, Augsburg, Germany

Background and Purpose: The principle of flow diversion has revolutionized the therapy of brain aneurysms. In this study, we report our experience of the new Surpass Evolve (SE) flow diverter in the treatment of intracranial aneurysms.
Materials and Methods: Inclusion criteria were patients suffering from wide-necked, blister-like, or fusiform/dissecting aneurysms in the anterior and posterior circulation who were treated with the SE as first-line therapy between May 2019 and June 2020 at two experienced institutions. Primary endpoint was technical success defined as favorable navigation to the target vessel and successful deployment of the SE. Secondary endpoints were favorable aneurysm occlusion defined as O'Kelly Marotta (OKM) scale C1-3+D on follow-up, procedure-related complications and retreatment.
Results: Forty-six aneurysms in 42 patients were treated with 57 SE flow diverters. Median aneurysm size was 6.6 mm (IQR 4.0–12.2 mm) with a median neck width of 4 mm (IQR 2.2–5.4 mm). Forty-one aneurysms (89 %) were located in the anterior circulation and six (13 %) were ruptured. The primary endpoint was reached in 96 %. Median follow-up was 116 days (IQR 92–134 days) and available for 36/46 (78 %) aneurysms. Favorable aneurysm occlusion was seen in 31/36 (86 %) aneurysms and 27/36 (75 %) were occluded completely. An acute in-stent thrombosis occurred in one (2 %) patient. Two aneurysms (6 %) required additional treatment due to insufficient closure.
Conclusion: The new SE flow diverter is safe and seems to be effective with promising occlusion rates at short-term follow-up.

[57] Endovascular Treatment of Intracranial Dural Arteriovenous Fistulas: A German Single Center Experience

Volker Maus[1], Finn Drescher[1], Lukas Goertz[2], Anushe Weber[1], Werner Weber[1], Sebastian Fischer[1]

[1]Department of Diagnostic and Interventional Neuroradiology and Nuclear Medicine, Universitätsklinikum Knappschaftskrankenhaus Bochum, Universitätsklinik der Ruhr-Universität Bochum
[2]Department of Neurosurgery, University Hospital of Cologne, Cologne, Germany

Background and Purpose: Intracranial dural arteriovenous fistulas (DAVFs) are abnormal shunts between dural arteries and dural venous sinus or cortical veins. The authors report their experience with endovascular therapy of primary complex DAVFs using modern embolic agents.
Methods: This is a retrospective analysis of patients with DAVFs treated between 2015 and 2019. Patient demographics and technical aspects including the use of embolic agent, access to the fistula, number of treatments, occlusion rates, and complications were addressed. Angiographic treatment success was defined as complete occlusion (CO) of the DAVF.
Results: Fifty patients were treated endovascularly. Median age was 61 years and 66 % were men. The most common symptom was pulsatile tinnitus in 17 patients (34 %). The most frequent location of the DAVF was transverse-sigmoid sinus (40 %). Thirty-six fistulas (72 %) had cortical venous reflux. Non-adhesive and adhesive liquid agents were used in 92 % as single material or in combination. Complete occlusion was achieved in 48 patients (96 %). In 28 individuals (56 %) only one procedure was necessary. Non-adhesive liquid agents were exclusively used in 14 patients (28 %) with CO attained in every case. For CO of tentorial DAVFs, multiple sessions were more often required than for the other locations (55 % vs. 14 %, $p = 0.0051$). Among 93 procedures, the overall complication rate was 3 %. The procedure-related mortality rate was 0 %.
Conclusion: Endovascular treatment of intracranial DAVFs is feasible, safe and effective with high rates of CO. In more than half of the patients the DAVF was completely occluded after a single procedure. However, in tentorial DAVFs, multiple sessions were more often required.

[58] Approaching the Boundaries of Endovascular Therapy in Acute Ischemic Stroke: Multi-Center Experience with Mechanical Thrombectomy in Vertebrobasilar Artery Branch Occlusions

Hanna Styczen[1], Sebastian Fischer[2], Leonard LL Yeo[3], Benjamin Yong-Qiang Tan[3], Christoph J. Maurer[4], Ansgar Berlis[4], Nuran Abdullayev[5], Christoph Kabbasch[5], Andreas Kastrup[6], Panagiotis Papanagiotou[7,8], Christin Clajus[9], Donald Lobsien[9], Eike Piechowiak[10], Johannes Kaesmacher[10,11], Volker Maus[2]

[1]Institute for Diagnostic and Interventional Radiology and Neuroradiology, University Hospital Essen, Essen, Germany
[2]Department of Radiology, Neuroradiology and Nuclear Medicine, Ruhr-University Bochum, Knappschaftskrankenhaus Langendreer, Bochum, Germany
[3]Division of Neurology, Department of Medicine, National University Health System, Singapore and Yong Loo Lin School of Medicine, National University of Singapore.
[4]Department of Diagnostic and Interventional Neuroradiology, University Hospital Augsburg, Augsburg, Germany

[5]Department of Diagnostic and Interventional Radiology, University Hospital Cologne, Cologne, Germany
[6]Department of Neurology, Klinikum Bremen, Bremen, Germany
[7]Department of Diagnostic and Interventional Neuroradiology, Klinikum Bremen-Mitte, Bremen, Germany
[8]Department of Neuroradiology, Aretaieion University Hospital, National and Kapodistrian University of Athens, Athens, Greece
[9]Department of Diagnostic and Interventional Radiology and Neuroradiology, Helios General Hospital Erfurt, Erfurt, Germany
[10]University Institute of Diagnostic and Interventional Neuroradiology, University Hospital Bern, Inselspital, University of Bern, Bern, Switzerland
[11]University Institute of Diagnostic and Interventional and Pediatric Radiology, University Hospital Bern, Inselspital, University of Bern, Bern, Switzerland

Background and Purpose: Little is known about catheter-based endovascular treatment of vertebrobasilar artery branch occlusion (VEBABO) in acute ischemic stroke (AIS). Nonetheless, the experience of mechanical thrombectomy (MT) in distal small sized arteries of the anterior circulation seems promising in AIS. In this multi-center study, we report feasibility, efficacy and safety of MT in VEBABO.
Methods: Retrospective analysis of consecutive AIS patients treated with MT due to VEBABO including posterior and anterior inferior cerebellar artery (PICA, AICA) and superior cerebellar artery (SCA) occlusions at seven tertiary care-centers between 01/2013–05/2020. Baseline demographics and angiographic outcomes including recanalization success of the affected cerebellar arteries and procedural complications were recorded. Clinical outcomes were evaluated by the modified Rankin Scale (mRS) at discharge and 90 days.
Results: Out of 668 endovascularly treated posterior circulation strokes we identified 16 (0.02 %) cases with VEBABO MT. Most frequently, MT of the SCA was done (13/16; 81 %). Most VEBABOs occurred after MT of initial basilar/posterior cerebral artery occlusion (9/16; 56 %). In 10/16 (63 %) procedures, the affected VEBABO was recanalized successfully. Three out of four patients (75 %) with isolated VEBABO had benefited from endovascular therapy. Subarachnoid hemorrhage was observed in 3/16 (19 %) procedures. The rate of favorable outcome (mRS 2) was 40 % at discharge and 47 % at 90 days follow-up. Mortality was 13 % (2/15).
Conclusion: Mechanical thrombectomy for VEBABO seems to be feasible and effective. However, the comparatively high rate of procedure-related hemorrhage highlights that the indication for MT in these occlusion sites should be weighed carefully.

[59] ASPECTS Interobserver Agreement of 100 Investigators from the TENSION Study

Noel van Horn, MD[1], Helge Kniep, Dipl.-Ing.[1], Gabriel Broocks, MD[1], Lukas Meyer, MD[1], Fabian Flottmann, MD[1], Matthias Bechstein, MD[1], Julia Götz, MD[1], Götz Thomalla, MD[2], Martin Bendszus, MD[3], Susanne Bonekamp, MD[3], Johannes Alex Rolf Pfaff, MD[3], Paulo Roberto Dellani, PhD[4], Jens Fiehler, MD[1], Uta Hanning, MHBA, MD[1]

[1]Department of Diagnostic and Interventional Neuroradiology, University Medical Center Hamburg Eppendorf, Hamburg, Germany
[2]Department of Neurology, University Medical Center Hamburg-Eppendorf, Hamburg, Germany
[3]Department of Neuroradiology, University of Heidelberg, Germany
[4]Forschungszentrum Jülich, Institute of Neurosciences and Medicine, Jülich, Germany

Background and Purpose: Evaluating the extent of cerebral ischemic infarction is essential for treatment decision and assessment of possible complications in patients with acute ischemic stroke. Patients are often triaged according to image-based early signs of infarction, defined by ASPECTS. Our aim was to evaluate interrater reliability in a large group of readers.
Methods: We retrospectively analyzed 100 investigators who independently evaluated 20 NCCT scans as part of their qualification program for the TENSION study. Test cases were chosen by four neuroradiologists who had previously scored CT scans with ASPECTS between 0 and 8 and high interrater agreement. Percent and interrater agreements were calculated for total ASPECTS, as well as for each ASPECTS region.
Results: Percent agreements for ASPECTS ratings was 28 %, with interrater agreement of 0.13 (CI95%: 0.09–0.16), at zero-tolerance allowance and 66 %, with interrater agreement of 0.32 (CI95%: 0.21–0.44), at tolerance allowance set by TENSION inclusion criteria. ASPECTS region with highest level of agreement was the insular cortex [percent agreement = 96 %, interrater agreement = 0.96 (CI95%: 0.94–0.97)] and with lowest level of agreement the M3 region [percent agreement = 68 %, interrater agreement = 0.39 (CI95%: 0.17–0.61)].
Conclusion: Despite relatively low exact interrater agreement for total ASPECTS, consensus for the decision for or against study enrollment was acceptable. Individual region analysis suggests some are particularly difficult to evaluate, with varying levels of reliability. Potential impairment of the supraganglionic region must be examined carefully, particularly in regard to the decision whether or not to perform mechanical thrombectomy.

[61] Accuracy of Nigrosome-1 Assessment and 18F-DOPA PET for Diagnosis of Parkinson's Disease in Patients with Neurodegenerative Parkinsonism

Daniel Kaiser*[1], Enrico Michler[2], Kiriaki Eleftheriadou[3], Jennifer Linn[1], Bjoern H. Falkenburger[3], Sebastian Hoberueck[2]

[1]Institut für Diagnostische und Interventionelle Neuroradiologie, Medizinische Fakultät Carl Gustav Carus, Technische Universität Dresden, Dresden, Germany
[2]Klinik und Poliklinik für Nuklearmedizin, Medizinische Fakultät Carl Gustav Carus, Technische Universität Dresden, Dresden, Germany
[3]Klinik und Poliklinik für Neurologie, Medizinische Fakultät Carl Gustav Carus, Technische Universität Dresden, Dresden, Germany

Background & Purpose: Visual radiological assessment of nigrosome-1 (N-1) on 3 T magnet resonance (MR) susceptibility-weighted imaging (SWI) shows a high diagnostic accuracy for Parkinson's disease (PD) versus control group[1]. Differentiation of PD from other diseases with similar clinical profile is difficult. We aimed to evaluate the accuracy of N-1 assessment as compared to 18F-DOPA positron emission tomography (PET) to diagnose PD in a highly pre-selected group of patients presenting with neurodegenerative parkinsonism in a tertiary referral center.
Methods: We enrolled consecutive patients who received 18F-DOPA PET-MR imaging with SWI between 01/2014 and 06/2019. PD versus non-PD parkinsonism was determined retrospectively according to the Movement Disorder Society (MDS) Clinical Diagnostic Criteria[2]. We performed a blinded visual assessment of N-1 for each hemi-mesencephalon as described previously and scans were divided accordingly in normal, abnormal and non-diagnostic[1]. We quantified 18F-DOPA uptake and classified as normal and abnormal using a set of spherical volumes of interest manually placed in bilateral basal ganglia and occipital reference. Sensitivity, specificity and predictive values of N-1 assessment, 18F-DOPA PET and the combined approach to PD detection were calculated.
Results: 50 patients (median age 65 (IQR 57.8, 74) years, 29 male, median duration of parkinsonism 2 (1, 4.5) years) met the inclusion criteria. Prevalence of PD according to MDS criteria was 38 % ($n = 19/50$ clinically established and probable PD). Table 1 shows the analysis of diagnostic accuracy.

Table 1 Diagnostic accuracy of N-1 assessment, 18F-DOPA PET and combined approach

n = 50, *n* = 19 with PD	N-1 Assessment	18F-DOPA PET	Combination
Sensitivity	81.8 %	86.4 %	77.3 %
Specificity	57.1 %	53.6 %	71.4 %
Positive predictive value	60 %	62.8 %	53 %
Negative predictive value	40.8 %	37.9 %	47,7 %
Accuracy	68 %	68 %	74 %

Conclusion: Diagnostic accuracy of N-1 assessment and 18F-DOPA PET were comparable. Interestingly, the combination of both methods slightly enhanced the accuracy.

References

1. Schwarz et al., The 'Swallow Tail' Appearance of the Healthy Nigrosome–A New Accurate Test of Parkinson's Disease: A Case-Control and Retrospective Cross-Sectional MRI Study at 3T, PLOS ONE, 2014, 9(4):e93814.
2. Postuma et al., MDS Clinical Diagnostic Criteria for Parkinson's Disease, Movement Disorders, 2015, 30(12):1591–1601.

[62] Impact of Thrombus Surface on Reperfusion Results in Basilar Artery Occlusion

Daniel Kaiser*[1], Pawel Krukowski[1], Volker Puetz[2], Jennifer Linn[1], Johannes C. Gerber[1]

[1]Institut für Diagnostische und Interventionelle Neuroradiologie, Medizinische Fakultät Carl Gustav Carus, Technische Universität Dresden, Dresden, Germany
[2]Klinik und Poliklinik für Neurologie, Medizinische Fakultät Carl Gustav Carus, Technische Universität Dresden, Dresden, Germany

Background & Purpose: Recently, we found an association of direct contact aspiration thrombectomy for middle cerebral artery occlusion and higher rates of successful first pass reperfusion in patients with a regular thrombus phenotype[1]. This study aimed to assess whether thrombus surface morphology has an impact on reperfusion results in thrombectomy of acute basilar artery occlusion (BAO).
Methods: We enrolled consecutive stroke patients treated by thrombectomy for acute BAO between 01/2016 and 12/2019. We assessed patients' characteristics, procedural data and thrombectomy results. We retrospectively categorized thrombus surface into regular versus irregular phenotype and analyzed first pass and final reperfusion and local recanalization results (modified treatment in cerebral ischemia (mTICI) and arterial occlusive lesion (AOL)) by blinded 3-reader-consensus as described before[1,2]. Data analysis was stratified according to thrombus phenotype.
Results: 100 patients (median age 74 (IQR 65, 80) years, 63 males, NIHSS 15 (5, 32), time from symptom onset to groin puncture 285 (190, 360) minutes) met the inclusion criteria. After consensus, 27 patients had a regular and 18 patients an irregular thrombus phenotype. Thrombus surface was not evaluable in 55 patients due to (1) poor delineation of thrombus surface secondary to bilateral inflow from vertebral arteries or early outflow via cerebellar collaterals, (2) stenosis, (3) spontaneous recanalization, (4) missing pretreatment images and (6) low-flow application of contrast medium to avoid vessel-rupture. Thrombectomy results according to thrombus phenotype are summarized in Table 1.
Conclusion: In BAO, thrombus surface phenotyping is poorly practicable. Nevertheless, regular phenotype was associated with the highest rates of successful reperfusion and local recanalization.

Table 1 Successful results of first pass and final reperfusion and local recanalization according to thrombus phenotype

Phenotype	First pass mTICI 2b–3, n(%)	Final mTICI 2b–3, n(%)	AOL 3, n(%)
Regular	14 (51.9)	24 (88.9)	19 (70.4)
Irregular	8 (44.4)	13 (72.2)	12 (66.7)
Non-evaluable	18 (32.7)	40 (72.7)	34 (61.8)

References

1. Kaiser et al., Impact of thrombus surface on first pass reperfusion in contact aspiration and stent retriever thrombectomy, Journal of NeuroIntervential Surgery, Published Online First: 11 June 2020, https://doi.org/10.1136/neurintsurg-2020-016194
2. Gerber et al., Efficacy and safety of direct aspiration first pass technique versus stent-retriever thrombectomy in acute basilar artery occlusion–a retrospective single center experience, Neuroradiology, 2017, 59:297–304

[64] Pitfalls in Stroke Imaging: Accidental Intra-Arterial Injection of Contrast in Brain CT Perfusion

Sondermann, Stefan; Schramm, Peter; Boppel, Tobias

Dept. of Neuroradiology, University Medical Center Schleswig-Holstein, Lübeck, Germany

Background & Purpose: CT perfusion is an important tool in stroke imaging, as it enables thrombectomy in cases with an unknown or extended time window by providing dynamic 4D-data to assess both penumbra and infarct core. We present a case with accidental intra-arterial injection of contrast to demonstrate the possible effects on brain CT perfusion imaging.
Methods: We present imaging findings of a stroke patient from our emergency department who was presenting with reduced vigilance and with a mild unilateral paresis that had resolved on arrival. Neurological examination was limited due to vigilance, patient history revealed a known paraplegia. Because of difficult conditions a peripheral venous catheter was placed cubital guided by ultrasound from an experienced emergency physician. Multimodal imaging including non-enhanced CT, CT angiography and CT perfusion was performed.
Results: CT perfusion showed an early enhancement of the posterior circulation vessels similar to the pattern of bilateral ACI occlusion, but with quick wash out followed by a normal attenuation curve of all

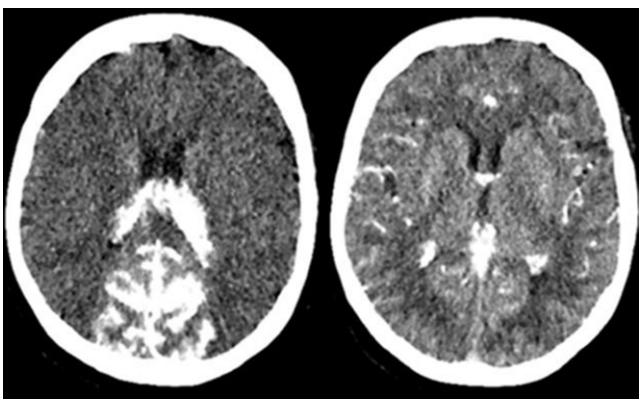

Fig. 1 Left: Second spiral of CT Perfusion (3 seconds). Enhancement of the posterior circulation with pattern similar to bilateral ACI occlusion. Right: Later spiral of the same CT Perfusion (24 seconds). Normal enhancement of anterior and posterior circulation.

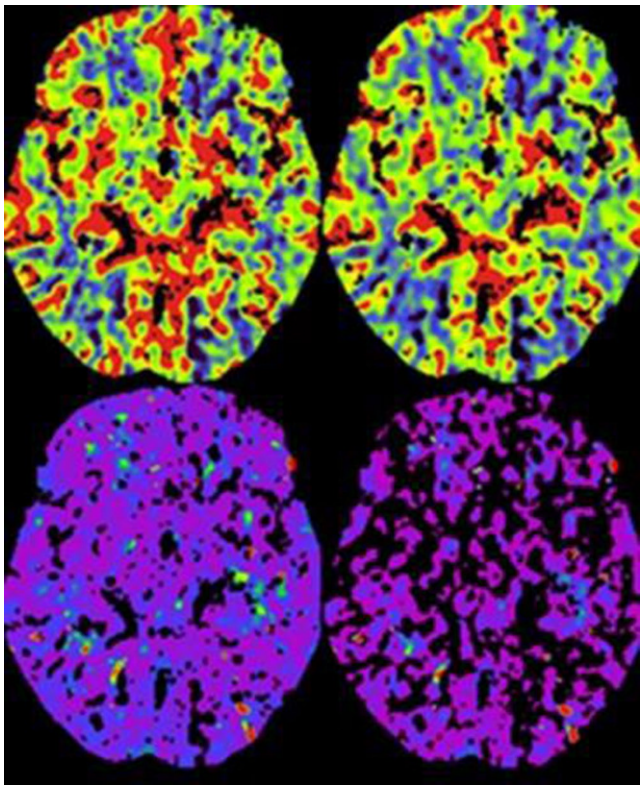

Fig. 2 Normal brain perfusion maps. Top left CBF, top right CBV, bottom left TTD, bottom right TMAX.

intracranial vessels. This was interpreted as rapid contrasting via brachial and vertebral artery with retrograde flow because of high injection rate followed by "normal" contrasting through venous circulation. Post-processing was possible because of quick wash out and no overlap between both phases of attenuation. The peripheral "venous" catheter was checked again and was found to be intra-arterial.

Conclusion: Accidental intra-arterial injection should be recognized immediately to prevent delay in the time sensitive setting of stroke imaging and to circumvent repetition without resolution of the underlying problem.

[65] Effect of Mechanical Thrombectomy on Clinical Outcome and Edema Progression in Patients with a Poor Collateral Profile

Gabriel Broocks MD[1], Andre Kemmling MD MHBA[2,3], Tobias D. Faizy MD[1,4], Matthias Bechstein MD[1], Lukas Meyer MD[1], Jens Fiehler MD[1], Helge Kniep Dipl.Ing[1*], Uta Hanning MD MHBA[1*]

[1]Department of Diagnostic and Interventional Neuroradiology, University Medical Center Hamburg-Eppendorf, Hamburg
[2]Department of Neuroradiology, Westpfalzklinikum, Kaiserslautern, Germany
[3]Department of Neuroradiology, University Medical Center Schleswig-Holstein, Lübeck, Germany
[4]Department of Radiology, Stanford University, Stanford, United States

Background and Purpose: The cerebral collateral circulation has an important impact on lesion progression and clinical outcome in ischemic stroke and may even modify the effect of endovascular treatment. The purpose of this study was to quantify the effect of vessel recanalization on lesion pathophysiology and clinical outcome in patients with a poor collateral profile.

Methods: 129 acute ischemic stroke patients with anterior circulation artery occlusion and a collateral score (CS) of 0–2 were included. Collateral profile was defined using an established 5-point scoring system in CT-angiography. Lesion progression was determined using quantitative lesion water uptake measurements in the admission and follow-up CT (FCT), and clinical outcome was assessed using modified Rankin Scales (mRS) scores after 90 days.

Results: In patients with persistent vessel occlusion, the mean mRS after 90 days was 5.2 (95 %CI: 4.6–5.7), which was significantly higher than in patients following successful vessel recanalization (mean mRS 4.0, 95 %CI: 3.7–4.4; $p<0.001$). Edema formation in FCT was significantly lower in patients with vessel recanalization versus persistent vessel occlusion (mean 19.5 %, 95 %CI: 17–22 % versus mean 27 %, 95 %CI: 25–29 %; $p<0.0001$).

Conclusion: Although poor collaterals are known to be associated with poor outcome, endovascular recanalization was still associated with significant edema reduction and comparably better outcome in this patient group. Patients with poor collaterals should not generally be excluded from thrombectomy.

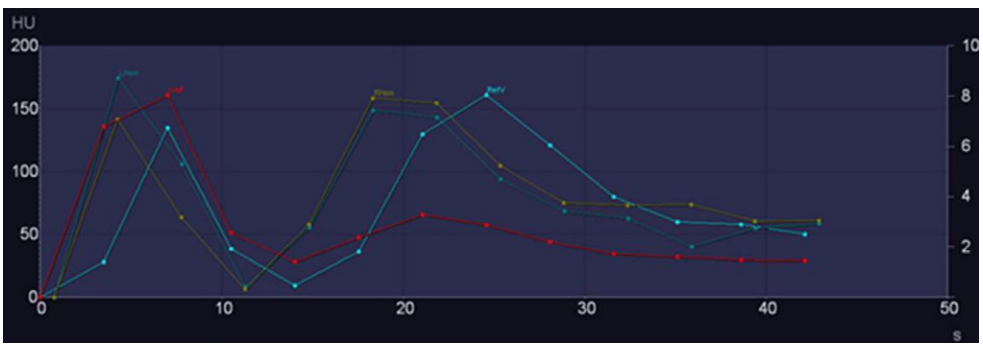

Fig. 3 Time attenuation curve via post-processing software with automatic vessel detection (syngo.via, Siemens Healthineers). Two peaks of contrast with the first around 3 to 6 seconds post injections and the second around 20 secons. Because there is no overlap manual post-processing was possible using only dara from later than the wash out of first peak

Fig. 1

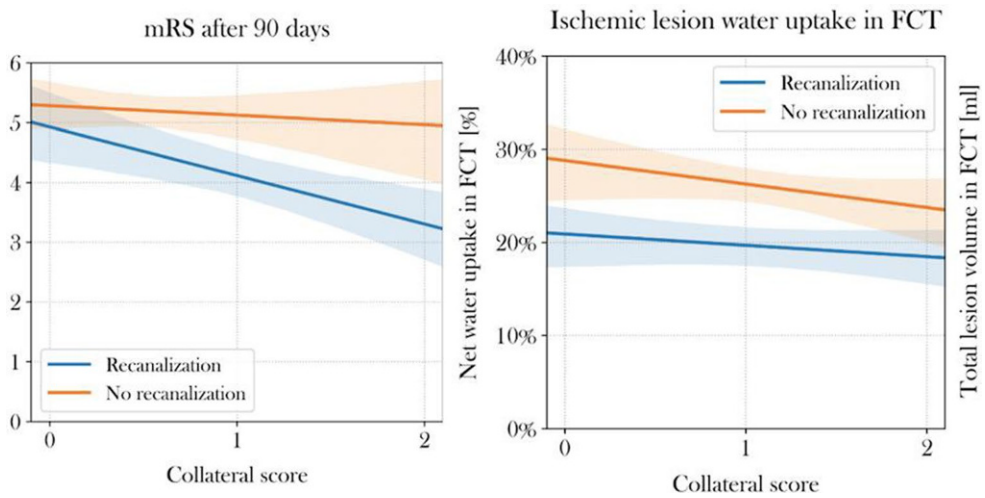

[66] Aneurysm Treatment in Acute SAH with Hydrophilic-Coated Flow Diverters Under Single-Antiplatelet Therapy

Lobsien D[1], Clajus C[1], Behme D[2], Ernst M[2], Riedel CH[2], Abu-Fares O[3], Götz FG[3], Fiorella D[4], Klisch J[1]

[1]Institute for Diagnostic and Interventional, Neuroradiology Helios Klinikum Erfurt, Erfurt
[2]Institute for Diagnostic and Interventional Neuroradiology University Medical Center Göttingen, Göttingen
[3]Institute for Diagnostic and Interventional Neuroradiology Hanover Medical School, Hanover
[4]Cerebrovascular Center at Stony Brook Hospital 101, Stony Brook

Background and Purpose: We report on our experience with ruptured intracranial aneurysms treated with flow diverters with hydrophilic coating (p48 and p64 MW HPC, phenox, Bochum, Germany) under single-antiplatelet therapy.
Methods: Patients were either treated with flow-diverter placement alone or flow-diverter and additional coiling. Due to the severity of the hemorrhage, the potential for peri-procedural re-hemorrhage and the potential for additional surgical interventions, a single-antiplatelet regimen was used in all of the patients.
Results: The majority of the patients received an ASA single antiplatelet protocol, one patient was treated with prasugrel only, one patient was treated with tirofiban first and then switched to the ASA single-antiplatelet protocol. One device related complication occurred in form of a thrombosis of an over-stented branch. All stents however remained open at DSA, CTA or MRA follow-up.
Conclusion: Single-antiplatelet therapy seems to be an option in carefully selected cases of SAH due to aneurysm rupture when the aneurysm cannot be treated otherwise.

Autorenindex